TECHNISCHE UNIVERSITÄT DRESDEN

Faculty of Forest, Geo and Hydro Sciences

Finite element method for coupled thermo-hydro-mechanical processes in discretely fractured and non-fractured porous media

Dissertation for awarding the academic degree
Doktoringenieur   (Dr.-Ing.)

Submitted by
M.Env.Sc. Norihiro Watanabe

Supervisor:

Mr. Prof. Dr.-Ing. Olaf Kolditz
Technische Universität Dresden

Mr. Prof. Dr.-Ing. habil. Heinz Konietzky
Technische Universität Bergakademie Freiberg

Leipzig, November 2011

Explanation of the doctoral candidate

This is to certify that this copy is fully congruent with the original copy of the dissertation with the topic:

„Finite element method for coupled thermo-hydro-mechanical processes in discretely fractured and non-fractured porous media"

…………………………………….….
Place, Date

…………………………………….….
Signature (surname, first name)

Finite Element Method for Coupled Thermo-Hydro-Mechanical Processes in Discretely Fractured and Non-fractured Porous Media

by

Norihiro Watanabe

A THESIS SUBMITTED IN PARTIAL FULFILLMENT OF THE REQUIREMENTS FOR THE DEGREE OF DOCTOR OF PHILOSOPHY IN ENGINEERING

Dresden University of Technology

October 2011

Abstract

Numerical analysis of multi-field problems in porous and fractured media is an important subject for various geotechnical engineering tasks such as the management of geo-resources (e.g. engineering of geothermal, oil and gas reservoirs) as well as waste management. For practical usage, e.g. for geothermal, simulation tools are required which take into account both coupled thermo-hydro-mechanical (THM) processes and the uncertainty of geological data, i.e. the model parametrization. For modeling fractured rocks, equivalent porous medium or multiple continuum model approaches are often only the way currently due to difficulty to handle geomechanical discontinuities. However, they are not applicable for prediction of flow and transport in subsurface systems where a few fractures dominates the system behavior. Thus modeling coupled problems in discretely fractured porous media is desirable for more precise analysis.

The subject of this work is developing a framework of the finite element method (FEM) for modeling coupled THM problems in discretely fractured and non-fractured porous media including thermal water flow, advective-diffusive heat transport, and thermoporoelasticity. Pre-existing fractures are considered. Systems of discretely fractured porous media can be considered as a problem of interacted multiple domains, i.e. porous medium domain and discrete fracture domain, for hydraulic and transport processes, and a discontinuous problem for mechanical processes. The FEM is required to take into account both kinds of the problems. In addition, this work includes developing a methodology for the data uncertainty using the FEM model and investigating the uncertainty impacts on evaluating coupled THM processes. All the necessary code developments in this work has been carried out with a scientific open source project OpenGeoSys (OGS).

In this work, fluid flow and heat transport problems in interactive multiple domains are solved assuming continuity of filed variables (pressure and temperature) over the two domains. The assumption is reasonable if there are no infill materials in fractures. The method has been successfully applied for several numerical examples, e.g. modeling three-dimensional coupled flow and heat transport processes in discretely fractured porous media at the Gross Schoenebck geothermal site (Germany), and three-dimensional coupled THM processes in porous media at the Urach Spa geothermal site (Germany).

To solve the mechanically discontinuous problems, lower-dimensional interface elements (LIEs) with local enrichments have been developed for coupled problems in a domain including pre-existing fractures. The method permits the possibility of using existing flow simulators and having an identical mesh for both processes. It enables us to formulate the coupled problems in monolithic scheme for robust computation. Moreover, it gives an advantage in practice that one can use existing standard FEM codes for groundwater flow and easily make a coupling computation between mechanical and hydraulic processes. Example of a 2D fluid injection problem into a single fracture demonstrated that the proposed method can produce results in strong agreement with semi-analytical solutions.

An uncertainty analysis of THM coupled processes has been studied for a typical geothermal reservoir in crystalline rock based on the Monte-Carlo method. Fracture and matrix are treated conceptually as an equivalent porous medium, and the model is applied to available data from the Urach Spa and Falkenberg sites (Germany). Reservoir parameters are considered as spatially random variables and their realizations are generated using conditional Gaussian simulation. Two reservoir modes (undisturbed and stimulated) are considered to construct a stochastic model for permeability distribution. We found that the most significant factors in the analysis are permeability and heat capacity. The study demonstrates the importance of taking parameter uncertainties into account for geothermal reservoir evaluation in order to assess the viability of numerical modeling.

Zusammenfassung

Die numerische Analyse von Mehrfeldproblemen in porösen und geklüfteten Medien ist ein wichtiges Thema für unterschiedliche geotechnische Aufgabenstellungen wie der wirtschaftlichen Nutzung von Georessourcen (z.B. Bewirtschaftung von geothermischen, Öl- und Gasreservoiren) oder der Verwahrung von Rückständen technischer Prozesse. Für die praktische Anwendung, z.B. im Bereich der geothermischen Energiegewinnung, werden Simulationsinstrumentarien benötigt, die sowohl thermisch-hydraulisch-mechanisch (THM) gekoppelte Prozesse als auch die Unsicherheiten geologischer Daten, die zu Problemen bei der Modellparametrisierung führen, berücksichtigen. Wegen der Schwierigkeiten bei der Beschreibung geomechanischer Diskontinuitäten kommen für die Modellierung von geklüftetem Gestein gegenwärtig vorrangig das Modell des äquivalenten porösen Kontinuums oder Mehrkontinua-Konzepte zur Anwendung. Diese Ansätze sind jedoch nicht für die Vorhersage von Fliess- und Transportproblemen in Untertagesystemen verwendbar, bei denen das Systemverhalten durch die Existenz mehrerer Klüfte dominiert wird. Somit ist eine präzisere Analyse von gekoppelten Prozessen in klüftig-porösen Medien anzustreben.

Gegenstand dieser Arbeit ist die Entwicklung eines spezifischen Konzepts für die Modellierung von gekoppelten THM-Problemen in geklüfteten und nicht geklüfteten porösen Medien im Rahmen der Finite-Element-Methode (FEM). Dieses Konzept soll die thermisch induzierte Porenwasserströmung, den advektiven und diffusiven Wärmetransport sowie thermo-poro-elastische Materialmodelle für die Gesteinsmatrix beinhalten. Vorbestehende Klüfte werden im Modell berücksichtigt. Die betrachteten Systeme von klüftig-porösen Medien können bezüglich der hydraulischen und Transportprozesse als Kombination interagierender, multipler Gebiete betrachtet werden (d.h. Gebiete poröser Medien und Gebiete separierter Klüfte), bezüglich der mechanischen Deformationsprozesse hingegen als Problemstellung mit Unstetigkeiten. Von relevanten FEM-Konzepten wird gefordert, dass sie beide Problemstellungen berücksichtigen. Zusätzlich beinhaltet diese Arbeit die Entwicklung einer Methodologie zur Behandlung von Datenunsicherheiten im Rahmen des FEM-Modells sowie die Untersuchung der Auswirkungen dieser Unsicherheiten auf die Analyse von gekoppelten THM-Prozessen. Die für die dargelegte Arbeit erforderlichen Softwareentwicklungen wurden im Rahmen des wissenschaftlichen open-source Projekts OpenGeoSys (OGS) umgesetzt.

Im Rahmen des präsentierten Konzepts wird für die Strömungs- und Wärmetransportprobleme in den interagierenden, multiplen Gebieten die Stetigkeit der Feldvariablen (Porendruck, Temperatur) über die Gebietsgrenzen hinweg vorausgesetzt. Diese Annahme ist physikalisch zweckmässig, wenn die Klüfte kein Füllmaterial enthalten. Die entwickelte Methode wurde erfolgreich in diversen numerischen Beispielen genutzt, wie etwa der Modellierung von dreidimensionalen, gekoppelten Strömungs- und Wärmetransportprozessen in klüftig-porösen Medien des Geothermie-Standorts Gross Schönebeck (Deutschland) und von räumlichen, gekoppelten THM-Vorgängen in porösen Medien des Geothermiestandorts Bad Urach (Deutschland).

Für die Lösung des diskontinuierlichen, geomechanischen Problems wurden Übergangselemente mit niedrig-dimensionierten Ansatzfunktionen (LIEs) sowie lokaler Anreicherung zur Simulation gekoppelter Probleme in Gebieten mit vorbestehenden Klüften entwickelt. Diese Vorgehensweise gestattet es, existierende Strömungsmodelle zu nutzen und die unterschiedlichen physikalischen Prozesse auf identischen Berechnungsgittern zu simulieren. Damit können die gekoppelten Modelle im Rahmen numerisch robuster, monolithischer Lösungskonzepte formuliert werden. Weiterhin kann in der numerischen Praxis der Vorteil genutzt werden, existierende FEM-Standardsoftware zu verwenden (die z.B. zur Modellierung von Grundwasserströmungen entwickelt wurde) und diese vergleichsweise unprob-

lematisch in ein gekoppeltes System zur Lösung geohydraulischer und geomechanischer Vorgänge zu integrieren. Am zweidimensional aufbereiteten Beispiel der Injektion eines Fluids in eine einzelne Kluft konnte gezeigt werden, dass das entwickelte Verfahren Ergebnisse generiert, die sehr gut mit semianalytischen Lösungen übereinstimmen.

Basierend auf dem Monte-Carlo-Verfahren wurden Unsicherheitsanalysen für gekoppelte THM-Prozesse für ein typisches Geothermie-Reservoir im kristallinen Gestein durchgeführt. Hierbei wurden Klüfte und Gesteinsmatrix konzeptionell als äquivalentes poröses Kontinuum betrachtet. Für die Studie standen Daten der Standorte Bad Urach und Falkenberg (Deutschland) zur Verfügung. Die Reservoirparameter wurden als Variablen mit zufälliger räumlicher Verteilung angesehen, die Berechnung der statistischen Realisierungen erfolgte auf der Basis von bedingten Gauss-Simulationen. Zwei Reservoirzustände (gestört und ungestört) wurden für die Generierung einer stochastischen Permeabilitätsverteilung untersucht. Es konnte festgestellt werden, dass Permeabilität und Wärmekapazität die Parameter mit dem grössten Einfluss auf die Berechnungsergebnisse darstellen. Diese Studie demonstrierte, dass die Berücksichtigung von Parameterunsicherheiten ein wichtiger Aspekt für die Realisierbarkeit numerischer Modelle im Bereich der Bewertung geothermischer Reservoire ist.

Contents

1 Introduction

1.1 Motivation

Numerical analysis of multi-field problems in porous and fractured media is an important subject for various geotechnical engineering tasks such as the management of geo-resources (e.g. engineering of geothermal, oil and gas reservoirs) as well as waste management (e.g. chemo-toxic and nuclear waste, CO_2 sequestration), see e.g. (Alonso et al., 2005; Doughty and Pruess, 2004; Stephansson et al., 2004). The use of computer modeling in the planning and management of the development of geothermal fields has become standard practice during the last decades. During that time models have been developed for more than 100 geothermal fields worldwide (Stephansson et al., 2004). Due to geological complexity and the number of processes involved, such as geometry, hydraulics, thermal effects, geochemical reaction and stress changes, simulation tools are required which take into account both coupled thermo-hydro-mechanical-chemical (THMC) processes and the uncertainty of geological data, i.e. the model parameterization (Noorishad et al., 1984; Tsang, 1991; Stephansson et al., 2004).

The analysis of coupled processes, in particular feedbacks of mechanical, thermal and geochemical effects to the flow system, is important for both hydrothermal (Clauser, 2003) and hot-dry-rock (HDR) systems (Bower and Zyvoloski, 1997; McDermott et al., 2006; Tsang, 1991). The behavior of HDR systems, particularly their fluid and heat transport characteristics, is affected by complex interactions among multiple physical and geochemical processes. HDR systems are designed to extract the heat energy stored in hot subsurface rocks by circulating fluids, often brine, through artificial or natural hydraulic pathways such as fractures or pores. Fluid injection causes large changes in pressure and temperature, thus inducing dynamic redistribution of in-situ stresses. This subsequently affects hydraulic properties such as permeability and porosity, due to geometrical changes of fractures and pore spaces. Thus the interactions take place vice versa between fluid and rock. Additional coupling occurs through pressure and temperature dependent fluid properties.

Any transport processes in subsurface systems are complicated when the fracture networks exist. Fractures provide the most likely pathway for the transmission of fluid, contaminants, and heat through the geologic underground. It is important to realize the interaction between the structure of the medium and the occurring physical processes within. Thus, the hydraulic behavior and the resulting transport of components as well as heat essentially depends on the structure of the fracture network, i.e. the connectivity of the fracture system. Moreover, the hydraulic properties of fractures strongly depend on the mechanical stress situation (Kolditz, 1997). The ordinary porous medium approach is frequently not applicable for prediction of flow and transport in fractured rock. More precise consideration of fracture geometries is required, although it is reasonable to choose carefully a limited number of major fractures which can adequately represent characteristics of the systems.

Furthermore, data uncertainty is one of the major problems in subsurface reservoir analysis. Direct borehole measurements are very limited due to technical issues and costs. Normally data are available from core samples and well bore logging for the local scale and geophysical measurements (e.g. microseismic monitoring) for a larger scale (e.g. Tenzer et al. (2000) for Urach Spa site and Weidler et al. (2002) for Soultz site). Thus, subsurface models are derived from limited information and include uncertainties. Dealing with uncertainty is a common necessity e.g. for safety assessment of nuclear waste repositories (Rautman and Treadway, 1991).

1.2 Previous research

Discussions about previous research are briefly presented below. More details about specific points are given in the corresponding sections.

Numerical THM models have been developed and applied to several HDR sites such as Soultz-sous-Foréts in the Rhine Valley (Kohl et al., 1995) and Urach Spa in the Swabian Alb (McDermott and Kolditz, 2006). More recently, chemical effects have been introduced into the coupled analysis (Kiryukhin et al., 2004; Kuhn, 2004; Taron et al., 2009; Taron and Elsworth, 2009). Of significant interest is the ability of dissolution and precipitation processes to alter pore structure and bulk reservoir permeability.

Models can be classified by their conceptualization of the fractured reservoir geometry (discrete fractures or fracture networks, equivalent porous media). Discrete fracture network (DFN) models are available for the simulation of fluid, mass and heat transport even for realistic geological structures, e.g. Bruel (1995); Kolditz (1995); Kolditz and de Jonge (2004) for the Soultz HDR reservoir. Their applicability in the context of fully coupled THM analysis, however, is still restricted to simplified problems (Walsh et al., 2008). Equivalent porous media approaches are used for THM analysis of fractured rock instead (Birkholzer et al., 2008) as well as THM modeling in geotechnics (Guimaraes et al., 2007; Kohlmeier, 2006).

From the mathematical point of view, THM processes lead to a non-linear coupled initial-boundary-value-problem which needs to be solved numerically for most of application cases. Among the available numerical methods, finite differences (FDM), volumes (FVM) and elements (FEM) are mainly used (de Boer, 2005; Borja and Aydin, 2004; Borsetto et al., 1981; Kohl, 1992; Lewis and Schrefler, 1998; Noorishad et al., 1984; Rutqvist et al., 2008). In addition, presence of fractures or faults in a domain of interest means one has to solve geomechanically discontinuous problems if the fractures are explicitly modeled. Treatment of such discontinuities makes it difficult for continuity based numerical methods, e.g. FDM, FEM, to simulate fully coupled THM problems in DFN models. Discontinuous methods, e.g. discrete element method (DEM), is one of the most attractive methods for modeling large displacements for moderately fractured rock masses where a large number of fractures have to be considered, or where large-scale displacements of individual blocks are possible (Cundall and Hart, 1992; Jing, 2003). Application of the DEM to coupled problems can be achieved by combining other continuous numerical methods. Solving fully coupled problems within the DEM has been studied in limited cases, e.g. no fluid is assumed in the rock matrix (Heinicke et al., 2009; Min et al., 2004; Wang and Konietzky, 2009).

Irrespective of the specific numerical method, the calculation of coupled THM problems is very expensive. This is mainly due to two reasons: degree of freedom (i.e. number of field variables) and strong coupling among non-linear processes. There are several ways to improve the computational efficiency, e.g. more efficient numerical algorithms, optimization of memory management in the code, and parallelization techniques. Among them, parallel computing provides the most powerful speed-up. Due to decreasing hardware cost in recent years, parallel computation is becoming very attractive for applied research (Schrefler et al., 2000; Shioya and Yagawa, 2005; Tezduyar and Sameh, 2006; Topping and Khan, 1996).

For HDR geothermal systems, aspects of uncertainty have been so far investigated in the framework of sensitivity analysis and parameters identification. Fractal and statistical DFN models have been developed, e.g. by Tezuka and Watanabe (2000). DFN models can represent the structural reservoir geology, but they are still restricted to simplified processes. Inversion methods have been used to identify physical rock parameters in order to reproduce the observed reservoir behavior (Lehmann et al., 1998).

1.3 Objective

Although numerous studies have been successfully achieved for modeling geothermal reservoir behavior, challenges still remain in terms of process coupling, conceptual modeling, data uncertainty, and computational efficiency as follows:

- Further investigation of geochemical (C) process, e.g. dissolution and precipitation, is important for evaluation of the long-term reservoir performance because of their impacts on hydraulic conductivity of the system.

- Modeling the mechanics related coupled problems in discretely fractured porous media, such as THM, is desirable to more focus on dominant players in the systems, i.e. hydraulically dominant fractures, for more precise analysis. Equivalent media or multiple continuum model approaches are often only the way currently due to difficulty to handle geomechanical discontinuities.

- Uncertainty in evaluation of HDR geothermal reservoirs has been partly investigated. Influence of data uncertainty on evaluating coupled THM problems in HDR geothermal reservoirs needs to be figured out.

- Improvement of the computation time is necessary to run a set of simulations to analyze the reservoir behavior, e.g. scenario-oriented analysis or probabilistic analysis.

Related with the above problems, this PhD work focuses on the following challenges:

(1) Development of the FEM for modeling coupled THM problems in discretely fractured porous media including thermal water flow, advective-diffusive heat transport, and thermoporoelasticity

(2) Monte-Carlo analysis of impacts of data uncertainty on THM coupled processes in a typical geothermal reservoir in crystalline rock

(3) Enhancement of computational efficiency for the Monte-Carlo analysis utilizing parallel computation on distributed memory systems

This work has a focus on the most important physical processes, i.e. THM. Geochemical effects will be explored in future work.

1.4 Numerical codes OpenGeoSys

This PhD work has been carried out with a scientific open source project OpenGeoSys (http://www.opengeosys.net). OpenGeoSys (OGS) aims the development of numerical methods for the simulation of THMC processes in porous and fractured media. OGS greatly relies on multi-dimensional FEM. The codes are implemented in C++, which is object-oriented with an focus on the numerical solution of coupled multi-field problems (multi-physics). Parallel versions of OGS are available relying on both MPI (Message Passing Interface) and OpenMP (Open Multi-Processing) concepts. Application areas of OGS are currently CO2 sequestration, geothermal energy, water resources management, hydrology, and waste deposition.

1.5 Dissertation structure

This dissertation is structured in the following. Section 2 explains the problem of interest in discretely fractured porous media and its mathematical model. Section 3 shortly describes the framework of the developed FEM. Section 4 demonstrates applications of the methods as well as the uncertainty analysis. Finally, summary and outlook are given in section 5. Publications produced by this work are included at the end.

2 Conceptual and mathematical model

2.1 Conceptual modeling of fractured rocks

Fractured rocks can be classified into different materials: *porous*, *fractured*, and *fractured porous media*. The conceptual model of a fractured porous medium reflects the occurrence and the significance of both discontinuities within rock (*fractures*) and *pore space* within the rock matrix. Fractures provide the most likely pathway for the transmission of fluid, contaminants, and heat through the geologic underground. Bear and Berkowitz (1987) distinguish between primary porosity (porosity of the rock matrix) and secondary porosity (porosity of fractures). The rock matrix can reveal a quite different hydraulic and transport behavior. Although the rock matrix may be impervious, or essentially impervious, to flow, it can play a primary role for retardation of contaminants or for heat storage. Finally, storage (due to porosity) and transfer (due to conductivity) are the essential properties of fractured rock which have to be described by appropriate models (Kolditz, 1997).

A conceptual model has to be chosen by the scale of the problem, the geological characteristics of the area of the investigation, and the purpose of the simulation (Dietrich et al., 2005). In general, following concepts exist for fractured rock model as illustrated in Figure 1.

- Discrete fracture model

- Continuum model (equivalent porous media)

- Multiple continuum model

- Hybrid model of discrete fracture and continuum models

Basic concepts are discrete fracture models, and continuum models (Kolditz, 1997). A discrete fracture model can be used if the considered processes are governed by the fractures alone. The continuum approach is applicable to fractured media as long as an representative elementary volume (REV) can be found for it.

The concept of the multi-continua approach was originally proposed by Barenblatt et al. (1960). This conceptual model is an extension of the ordinary single-continuum approach for the case of strongly heterogeneous media such as fractured rocks. For this purpose, the heterogeneous medium is subdivided into multiple interacting homogeneous subsystems (e.g. one representing the fracture network and the other for the rock matrix). In fact, the multi-continua model presumes the existence of a REV which is common to all subsystems. This approach is definitely advantageous for expressing the different characteristics of fractures and rock matrix. The fracture continuum covers the conductive part, whereas the matrix continuum regards to the storage capacity of the whole domain. The multi-continua approach deals with a situation where the hydraulic and/or transport systems are not in an equilibrium state at the microscopic scale. Exchange processes take place between the solid and the fluid phases, or between zones of mobile and immobile groundwater in layered aquifers, or even between fractures and rock matrix in fractured porous aquifers.

The hybrid model for a fractured porous medium is coupling the two basic concepts which specially account for exchange processes between fractures and the enclosed rock matrix. This hybrid approach implies the possibility of homogenization of the rock matrix at a macroscopic scale (i.e. the characteristic length scale of fractures). The term rock matrix denotes a quite heterogeneous medium at a microscopic scale which is interweaved by numerous microfissures and pores. It is assumed, however, that these microstructures are well connected, and thus, the hydraulic and transport characteristics of the rock matrix
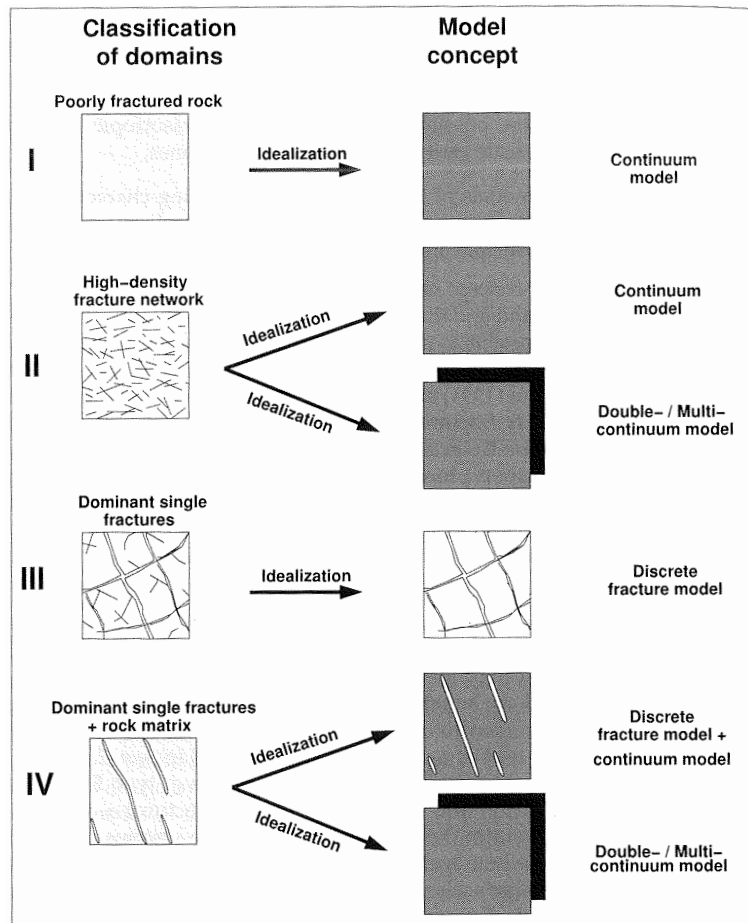
Figure 1: Model concepts for the description of fractured porous media (Dietrich et al., 2005)

can be described by averaged quantities, i.e. the continuum approach of a porous medium can be applied (Kolditz, 1997).

This work focuses on a subsurface system where high conductive and long fractures sparsely distribute in background rock matrices. Both the fractures and rock matrices are filled with groundwater, i.e. saturated conditions. One can describe groundwater flow in the system by considering a combination of discrete fractures as hydraulic conduits, and rock matrices as porous media, respectively (Guvanasen and Chan, 2000; Baca et al., 1984; Dietrich et al., 2005; Woodbury and Zhang, 2001; Segura and Carol, 2004). This is based on an assumption that groundwater in the discrete fractures dominantly flows along the fracture plane. In addition, it is assumed that the domain is composed of continuous porous medium blocks with embedded connected planes representing the discrete fractures (Guvanasen and Chan, 2000).

2.2 Mathematical modeling of coupled THM processes

The physical system incorporates non-isothermal liquid flow in a deforming porous medium connected with discontinuities, i.e. discrete fractures. Local equilibrium of thermodynamics is assumed and macroscopic balance equations are considered to derive the governing equations. Macroscopic hydro-mechanical (HM) behavior of the system is described by the Biot's consolidation theory and its extension to discrete fractures. More details on THM mechanics for porous media can be found e.g. in Coussy (2004); Ehlers and Bluhm (2002); Lewis and Schrefler (1998), and for discretely fractured porous media, e.g. in Noorishad and Tsang (1996); Guvanasen and Chan (2000); Rutqvist and Stephansson (2003).

Discrete fractures are conceptualized in a different way depending on which process is considered. In hydraulic and transport process, discrete fractures can be idealized as lower-dimensional geometries, e.g. lines in two-dimensional space. This implies that fluid pressure or temperature is uniform across the fracture width. In mechanical process, the fractures can be considered as a pair of surfaces between which normal and shear displacements are permissible.

In the following sections, details of each process are presented. To describe mathematical models, one can explain them with focusing on each physical process whereas others would focus on each medium, i.e. porous media or fractures. In order to more clearly explain about interaction between porous media and discrete fractures, the former is taken in the following. The corresponding field variables are liquid phase pressure p, temperature T, and solid displacement vector $\mathbf{u}$. We use superscripts l and s to indicate the liquid phase and the solid phase in porous media, and m and f to indicate porous media and discrete fractures, respectively.

2.3 Hydraulic process

2.3.1 Porous medium

Mass conservation law Fluid flow in deformable and saturated porous media is described by the following volume balance equation based on mass balance equations of both liquid and solid phases in porous medium,

$$S_s \frac{\partial p}{\partial t} - \beta \frac{\partial T}{\partial t} + \nabla \cdot \mathbf{q}_H + \alpha \nabla \cdot \frac{\partial \mathbf{u}}{\partial t} = Q_H \tag{1a}$$

where $S_s = (\alpha - n)/K^s + n/K^l$ is the constrained specific storage of the medium with α the Biot-Willis coefficient for the porous medium, n porosity, K^s the compressibility of solid

and K^l the compressibility of liquid. $\mathbf{q}_H$ is the volumetric Darcy flux, $\beta = (\alpha - n)\beta^s + n\beta^l$ is the thermal expansion coefficient, and Q_H is fluid source/sink term representing the effect of a fluid exchange with the fractures, or fluid extraction (injection) from a wellbore. The specific storage comprises a mechanical alteration in response to pressure. Volumetric change of pore space due to change in the stress field is expressed as $\nabla \cdot (\partial \mathbf{u}/\partial t)$.

Darcy's law   When the flow is assumed to follow the Darcy's law, the volumetric flux $\mathbf{q}_H$ is

$$\mathbf{q}_H = \frac{\mathbf{k}}{\mu}(-\nabla p + \rho^l \mathbf{g}) \tag{1b}$$

where $\mathbf{k}$ is intrinsic permeability tensor, μ is fluid dynamic viscosity, ρ^l is fluid density, and $\mathbf{g}$ is the gravitational acceleration vector.

2.3.2   Discrete fracture

Mass conservation law   Assuming no infill materials in fractures, the volume balance equation for the discrete fracture can be described in its local coordinates from the mass balance law as

$$b_m S_s \frac{\partial p}{\partial t} + \alpha \frac{\partial b_m}{\partial t} + \bar{\nabla} \cdot (b_h \, \bar{\mathbf{q}}_H) - \beta \frac{\partial T}{\partial t} + q_H^+ + q_H^- = 0 \tag{2a}$$

where b_m and b_h denotes a mechanical and hydraulic (hydraulically effective) aperture, respectively. $S_s = \alpha/K^l$, $\beta = \alpha\beta^l$ are specific storage, thermal expansion coefficient for a fracture, respectively. $\bar{\nabla}$ is the divergence operator in local coordinate systems. q_H^+ and q_H^- are the leakage flux from each side of the fracture surfaces to the surrounding porous media. The volumetric change of unit space due to change in the stress field is expressed as $\partial b/\partial t$.

Parallel plate concept   The parallel plate concept can be applied when the flow is laminar and the fracture is considered as a uniform plate (Snow, 1969; Zimmerman and Bodvarsson, 1996). For detailed studies regarding non-linear flow in fractures, and thus violations to Darcys law, please refer to the literature (Kolditz, 2001). The flux equation in unit volume for the discrete fracture is defined as

$$\bar{\mathbf{q}}_H{}^f = \frac{b_h^2}{12\mu}\bar{\mathbf{I}}(-\bar{\nabla}p^f + \rho^l \mathbf{g}). \tag{2b}$$

where $\bar{\mathbf{I}}$ is the unit tensor assuming isotropic permeability. We can see that in equation (2a) the volumetric change of unit space due to change in the stress field is expressed as $\partial b/\partial t$, while the permeability tensor in equation (2b) is given by the cubic law. The equations above denote that the fracture aperture b has impact on the volumetric change of space and also the hydraulic conductivity. Thus the flow equations are nonlinear when variation of the fracture aperture is not negligible for the flow system.

2.4   Thermal process

2.4.1   Porous medium

Energy balance   The energy balance equation for heat transport in porous media is given as

$$c_p \rho \frac{\partial T}{\partial t} + \nabla \cdot \mathbf{q}_\mathrm{T} = Q_\mathrm{T} \tag{3a}$$

where $c_p\rho = nc_p^l\rho^l + (1-n)c_p^s\rho^s$ is heat storage of porous medium with n porosity, c_p^l specific heat capacity of fluid, c_p^s specific heat capacity of rock and ρ^s rock density. $\mathbf{q}_{\mathrm{T}}$ is heat flux, and Q_T is source/sink term including the effect of a heat exchange with the fractures.

Heat flux Considering advective and diffusive mechanism, heat flux $\mathbf{q}_{\mathrm{T}}$ is described as

$$\mathbf{q}_{\mathrm{T}} = -\lambda\nabla T + c_p^l\rho^l\mathbf{q}_H\,T \tag{3b}$$

where $\lambda = n\lambda^l + (1-n)\lambda^s$ is heat conductivity of porous medium with λ^l heat conductivity of fluid, λ^s heat conductivity of rock. $\mathbf{q}_H$ denotes the Darcy flux.

2.4.2 Discrete fracture

Energy balance The energy balance equation for heat transport in the discrete fracture is

$$b_m c_p^l\rho^l\frac{\partial T}{\partial t} + \bar{\nabla}\cdot\bar{\mathbf{q}}_{\mathrm{T}} + q_T^+ + q_T^- = 0 \tag{4a}$$

where $\bar{\mathbf{q}}_{\mathrm{T}}$ is heat flux and Q_{T} is heat source/sink term. q_T^+ and q_T^- are the leakage heat flux from each side of the fracture surfaces to the surrounding porous media.

Heat flux The advective and diffusive heat flux $\bar{\mathbf{q}}_{\mathrm{T}}$ is defined as

$$\bar{\mathbf{q}}_{\mathrm{T}} = -b_m\lambda^l\bar{\nabla}T + b_h c_p^l\rho^l\bar{\mathbf{q}}_H\,T. \tag{4b}$$

Notice that mechanical aperture b_m is used to calculate the volumetric flux with respect to fluid volume, i.e. caused by diffusion mechanism, whereas b_h is used with respect to fluid movement, i.e. caused by advection mechanism.

2.5 Mechanical process

2.5.1 Concept of effective stress

In porous media and fractures saturated with liquids, the main characteristics of the solid phase constitutive relation can be written in terms of the effective stress $\boldsymbol{\sigma}'$. The effective stress $\boldsymbol{\sigma}'$ is defined as

$$\boldsymbol{\sigma}' = \boldsymbol{\sigma} + \alpha p\mathbf{I} \tag{5}$$

where $\mathbf{I}$ is the unit tensor. The Biot's constant is introduced in the equation in order to account for the deformability of the solid grains. The Biot's constant is given as

$$\alpha = 1 - \frac{K_T}{K_s} \tag{6}$$

with the bulk modulus of the skeleton K_T and of the grain material K_s. $\alpha = 1$ for incompressible grains ($1/K_s \approx 0$).

9

2.5.2 Porous medium

Stress equilibrium Non-isothermal consolidation of porous media with slowly moving fluids can be considered as a quasi-static stress equilibrium problem. The linear momentum balance equation in the terms of stress tensor can be written as

$$\nabla \cdot (\boldsymbol{\sigma}' - \alpha p \mathbf{I}) + \rho \mathbf{g} = 0 \tag{7a}$$

The density of the porous medium is composed by two phases, liquid and solids $\rho = n\rho^l + (1-n)\rho^s$.

Constitutive law The constitutive law for stress-strain behavior including the thermo elasticity is defined as

$$d\boldsymbol{\sigma}' = \mathbb{C} \left(d\boldsymbol{\epsilon} - \alpha_T \Delta T \mathbf{I} \right) \tag{7b}$$

with $\mathbb{C}$ a forth-order material tensor, $\boldsymbol{\epsilon}$ the total strain, α_T thermal expansion coefficient and ΔT temperature increment. For nonlinear, generalized analysis, equation (7b) is written in an incremental form with the material tensor $\mathbb{C}$. The isotropic elasticity tensor $\mathbb{C}$ is,

$$\mathbb{C} := \lambda \delta_{ij} \delta_{kl} + 2G \delta_{ik} \delta_{jl} \tag{7c}$$

where δ is the Kronecker delta, $G = E/(2(1+\nu))$ shear modulus with Young's modulus E and Poisson ratio ν. $\lambda = 2G\nu/(1-2\nu)$ is the so called Lamé constant.

Strain-displacement relationship Assuming small deformation, the kinematics is described by

$$\boldsymbol{\epsilon} = \frac{1}{2}(\nabla \mathbf{u} + (\nabla \mathbf{u})^T) = \nabla^s \mathbf{u} \tag{7d}$$

where superscript T means the transpose of the matrix. Displacement vector $\mathbf{u}$ is the primary variable to be solved by substituting the constitutive law.

2.5.3 Discrete fractures

Fracture relative displacement A discrete fracture can be approximated by a pair of surfaces between which normal and shear displacements are permissible. Displacement difference between two sides of the surfaces is defined as a *fracture relative displacement*. In a local coordinate system of the fracture plane, the *local* relative displacement $\mathbf{w}$ is given as

$$\mathbf{w} = \left\{ \begin{array}{c} w_{\mathrm{t}} \\ w_{\mathrm{n}} \end{array} \right\} = \left\{ \begin{array}{c} u_{\mathrm{t}}^+ - u_{\mathrm{t}}^- \\ u_{\mathrm{n}}^+ - u_{\mathrm{n}}^- \end{array} \right\} \tag{8a}$$

where subscripts t and n denote tangential and normal directions to the fracture plane, respectively. Superscripts $+$ and $-$ indicate one side of the surfaces and the other side, respectively. The local relative displacement can be written with the one in a global coordinate system $[\![\mathbf{u}]\!]$, which is the *global* relative displacement, as

$$\mathbf{w} = \mathbf{R} \, [\![\mathbf{u}]\!] \tag{8b}$$

$$\mathbf{R} = \left[\begin{array}{cc} \cos\theta & \sin\theta \\ -\sin\theta & \cos\theta \end{array} \right] \tag{8c}$$
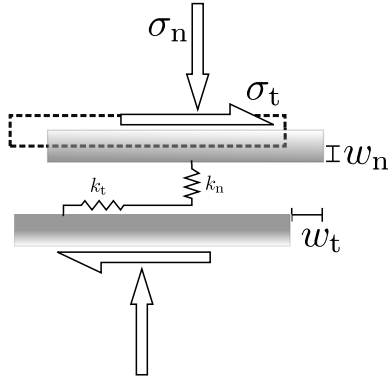
10

Figure 2: Discrete fracture model

where $\mathbf{R}$ is a rotation matrix transforms global coordinates to the local coordinates in two-dimensional space with an angle θ. Hence a change of a fracture aperture b, which is one of the key parameters characterizing the flow in the fracture, can be expressed with either $\mathbf{w}$ or $[\![\mathbf{u}]\!]$ as

$$\Delta b = \mathbf{m}^{f^T} \mathbf{w} = \mathbf{m}^{f^T} \mathbf{R} [\![\mathbf{u}]\!] \tag{8d}$$

with the mapping vector $\mathbf{m}^f = \{0, 1\}^T$.

Stress equilibrium The HM equilibrium conditions in the fracture are governed by fracture mechanical stresses and liquid pressure between the surfaces as

$$\boldsymbol{\sigma}^f = \boldsymbol{\sigma}'^f - \alpha \, \mathbf{m}^f \, p \tag{8e}$$

where $\boldsymbol{\sigma}^f = \{\boldsymbol{\sigma}_t^f, \boldsymbol{\sigma}_n^f\}^T$ is the total stress vector applied on the fracture plane in tangential and normal directions. Similar to poroleasticity theory, $\boldsymbol{\sigma}'^f$ is the effective stress, and p^f is the liquid pressure in the fracture.

Constitutive law Relationship between the effective stress and the fracture relative displacement is described by the stiffness tensor $\mathbf{K}$ as

$$\mathrm{d}\boldsymbol{\sigma}'^f = \mathbf{K} \, \mathrm{d}\mathbf{w} \tag{8f}$$

$$\mathbf{K} = \begin{bmatrix} k_{\mathrm{tt}} & k_{\mathrm{tn}} \\ k_{\mathrm{nt}} & k_{\mathrm{nn}} \end{bmatrix} \tag{8g}$$

where k_{tt} and k_{nn} are the joint shear and normal stiffness, respectively. k_{tn} and k_{nt} govern coupling effects between normal and shear displacements. Often the joint stiffness coefficients are nonlinear about normal and shear stress applied on the fracture plane. Commonly used fracture closured laws are, for example, Goodman's hyperbolic model and the Barton-Bandis model (Rutqvist and Stephansson, 2003).

3 Finite element method

3.1 Introduction

In this section, application of the finite element method (FEM) to coupled THM problems in discretely fractured porous media is presented. Modeling concept and partial differential equations to be solved are already described in the previous chapter. Related numerical methods such as coupling procedures and parallelization are also shortly presented to give an overview of numerical analysis utilizing the FEM.

3.2 Representation of discrete fractures and porous media

The ability to handle non-uniform and distorted computational domains has been one of attractive features of the FEM. The geometric object can be represented by a mesh of 1-D, 2-D and/or 3-D basic elements (geometric units) such as lines, triangles, quadrilaterals, tetrahedrons, hexahedra and pyramids. Which type of element is most appropriate for a particular problem depends on several factors, such as domain geometry, required accuracy, computational costs etc (Kolditz, 2002).

Domains composed of discrete fractures and porous media can be discretized by combination of multiple element types (Table 1). In most cases, discrete fractures can be idealized as lower-dimensional geometric objects so that they can be represented by, for example, lines in two-dimensional space. If solutions are assumed to be continuous over domains of the fractures and porous media, the discrete fracture elements must be located on edges of porous medium elements and both kind of elements share the same nodes. Example of a numerical mesh is shown for Grimsel fracture network in three-dimensional space in Figure 3. The geometric data is provided by the German Federal Institute for Geosciences and Natural Resources (BGR). Discrete fractures are represented by triangle elements and surrounded by tetrahedral elements as porous media. Often mesh refinement is required near the fractures due to appearance of steep gradient of solutions.

Table 1: Element types for discretely fractured porous media

Space	Element type	
	Porous media	Discrete fractures
2D	tetrahedral, hexahedral, prismatic	triangle, quadrilateral
3D	triangle, quadrilateral	lines

3.3 Weak formulation

The Method of Weighted Residuals (MWR) and the Green's theorem are applied to derive weak formulations of the governing equations given in the previous section. The weak forms for the volume balance equations (1a),(2a), the energy balance equations (3a),(4a) and the momentum balance equation (7a) can be written as below respectively,

Hydraulic process

$$\int_{\Omega} \omega S_s \frac{\partial p}{\partial t} \, d\Omega + \int_{\Omega} \boldsymbol{\omega}^{\mathrm{T}} \alpha \nabla \cdot \frac{\partial \mathbf{u}}{\partial t} \, d\Omega + \int_{\Omega} \omega \beta \frac{\partial T}{\partial t} \, d\Omega - \int_{\Omega} \nabla \omega^{\mathrm{T}} \cdot \mathbf{q}_H \, d\Omega$$

12
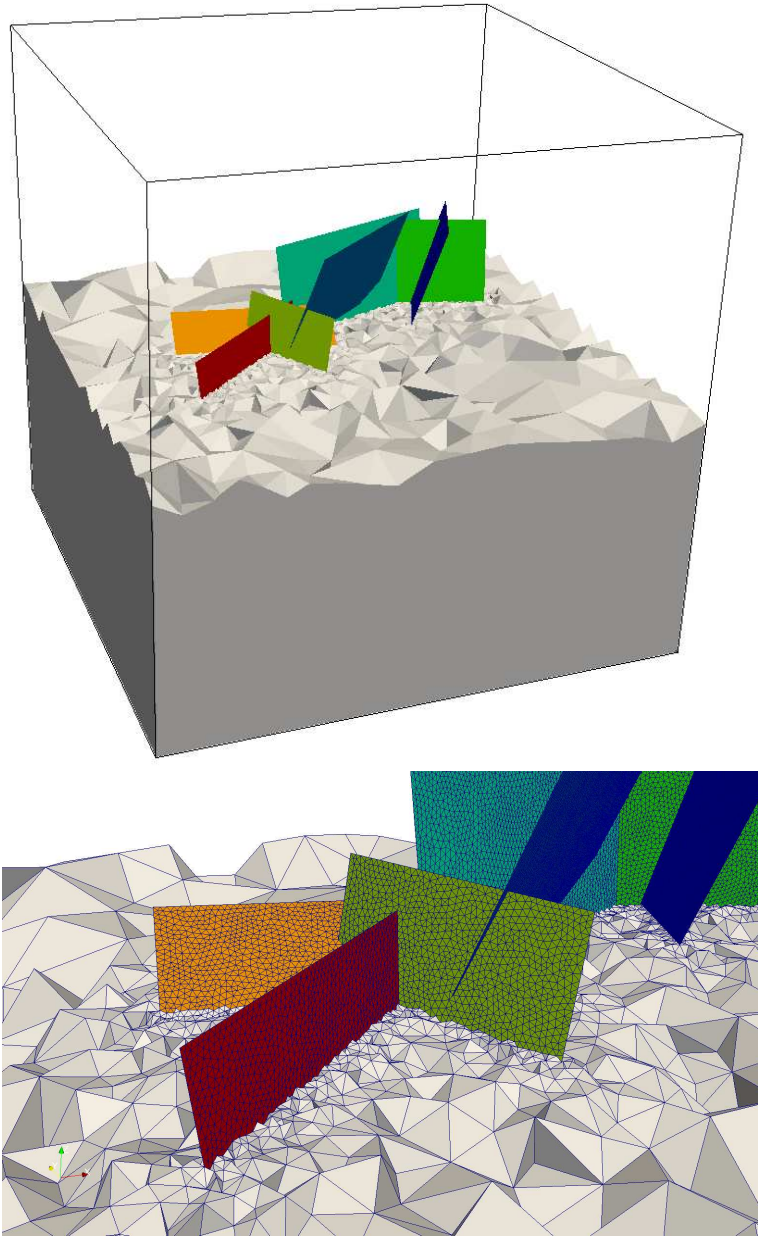
Figure 3: Example of a mesh for discretely fractured porous media: overall view (top) and enlarged in vicinity of fracture networks (bottom)

$$+\int_{\Gamma_H^q} \omega \, (\mathbf{q}_H \cdot \mathbf{n}) \, \mathrm{d}\Gamma - \int_\Omega \omega \, Q_H \, \mathrm{d}\Omega = 0 \tag{9a}$$

$$\int_{\Gamma_\mathrm{d}} \omega \, b_m S_s \frac{\partial p}{\partial t} \, \mathrm{d}\Gamma + \int_{\Gamma_\mathrm{d}} \omega \alpha \frac{\partial b_m}{\partial t} \, \mathrm{d}\Gamma + \int_{\Gamma_\mathrm{d}} \omega \beta \frac{\partial T}{\partial t} \, \mathrm{d}\Gamma - \int_{\Gamma_\mathrm{d}} \nabla \omega^\mathrm{T} \cdot (b_h \mathbf{q}_H) \, \mathrm{d}\Omega$$
$$+ \int_{\Gamma_H^q} \omega \, b_h (\mathbf{q}_H \cdot \mathbf{n}) \, \mathrm{d}\Gamma + \int_{\Gamma_\mathrm{d}} \omega \, q_H^+ \, \mathrm{d}\Gamma + \int_{\Gamma_\mathrm{d}} \omega \, q_H^- \, \mathrm{d}\Gamma = 0 \tag{9b}$$

Heat transport process

$$\int_\Omega \omega c_p \rho \frac{\partial T}{\partial t} \, \mathrm{d}\Omega + \int_\Omega \omega c_p \rho \, \mathbf{q}_H \cdot \nabla T \, \mathrm{d}\Omega - \int_\Omega \nabla \omega^\mathrm{T} \cdot (-\lambda \nabla T) \, \mathrm{d}\Omega$$
$$+ \int_{\Gamma_T^q} \omega \, (-\lambda \nabla T \cdot \mathbf{n}) \, \mathrm{d}\Gamma - \int_\Omega \omega^\mathrm{T} Q_\mathrm{T} \, \mathrm{d}\Omega = 0 \tag{10a}$$

$$\int_{\Gamma_\mathrm{d}} \omega \, b_m c_p^l \rho^l \frac{\partial T}{\partial t} \, \mathrm{d}\Gamma + \int_{\Gamma_\mathrm{d}} \omega c_p^l \rho^l \, b_h \mathbf{q}_H \cdot \nabla T \, \mathrm{d}\Gamma - \int_{\Gamma_\mathrm{d}} \nabla \omega^\mathrm{T} \cdot (-b_m \lambda^l \nabla T) \, \mathrm{d}\Gamma$$
$$+ \int_{\Gamma_T^q} \omega \left(-b_m \lambda^l \nabla T \cdot \mathbf{n} \right) \, \mathrm{d}\Gamma + \int_{\Gamma_\mathrm{d}} \omega \, q_T^+ \, \mathrm{d}\Gamma + \int_{\Gamma_\mathrm{d}} \omega \, q_T^- \, \mathrm{d}\Gamma = 0 \tag{10b}$$

Mechanical process

$$\int_\Omega \nabla^s \boldsymbol{\omega}^\mathrm{T} : (\boldsymbol{\sigma}' - \alpha p \mathbf{I}) \, \mathrm{d}\Omega - \int_\Omega \boldsymbol{\omega}^\mathrm{T} \cdot \rho \mathbf{g} \, \mathrm{d}\Omega - \int_{\Gamma_t} \boldsymbol{\omega}^\mathrm{T} \cdot \bar{\mathbf{t}} \, \mathrm{d}\Gamma$$
$$- \int_{\Gamma_\mathrm{d}} \boldsymbol{\omega}^{+\mathrm{T}} \cdot \mathbf{t}_\mathrm{d}^+ \, \mathrm{d}\Gamma - \int_{\Gamma_\mathrm{d}} \boldsymbol{\omega}^{-\mathrm{T}} \cdot \mathbf{t}_\mathrm{d}^- \, \mathrm{d}\Gamma = 0 \tag{11}$$

Here $\omega \in \mathcal{V}^1 \subset H_\Gamma^1(\Omega)^1$ is the linear test function, and $\boldsymbol{\omega} \in \mathcal{V}^\mathrm{n} \subset H_\Gamma^1(\Omega)^\mathrm{n}$ is the quadratic test function in n dimensional space. Ω denotes the model domain with Γ as domain boundary, where boundary conditions have to be specified for all field functions p, T, and $\mathbf{u}$, respectively. $\mathbf{t}_\mathrm{d}^+$, $\mathbf{t}_\mathrm{d}^-$ are traction vectors applied on two sides of a fracture plane d. Assuming continuity of the traction force at the fracture plane

$$\mathbf{t}_\mathrm{d}^+ = -\mathbf{t}_\mathrm{d}^- , \tag{12}$$

the weak form (11) can be written as

$$\int_\Omega \nabla^s \boldsymbol{\omega}^\mathrm{T} : (\boldsymbol{\sigma}' - \alpha p \mathbf{I}) \, \mathrm{d}\Omega - \int_\Omega \boldsymbol{\omega}^\mathrm{T} \cdot \rho \mathbf{g} \, \mathrm{d}\Omega - \int_{\Gamma_t} \boldsymbol{\omega}^\mathrm{T} \cdot \bar{\mathbf{t}} \, \mathrm{d}\Gamma$$
$$+ \int_{\Gamma_\mathrm{d}} [\![\boldsymbol{\omega}]\!]^\mathrm{T} \cdot \mathbf{t}_\mathrm{d}^- \, \mathrm{d}\Gamma = 0 \tag{13}$$

where $[\![\boldsymbol{\omega}]\!] = \boldsymbol{\omega}^+ - \boldsymbol{\omega}^-$ denotes jump of the test function at discontinuities. The traction force $\mathbf{t}_\mathrm{d}^-$ can be expressed by the stress in a fracture (8e).

14

3.4 Galerkin finite element method

The basic steps in the finite element approximation are (1) domain discretization by finite elements, (2) discretization of the integral (weak) formulations of the PDEs, and (3) generation of interpolation functions to approximate the unknown values of field variables. Domain discretization is already mentioned in the previous section.

We use the standard Galerkin method to spatially discretize the weak forms (9a),(9b), (10a), (10b), (11) of the THM balance equations. Primary variables of the multi-field problem are liquid phase pressure p, temperature T, and displacement vector $\mathbf{u}$ (fracture relative displacement $[\![\mathbf{u}]\!]$). All variables are approximated by admissible interpolation functions in the Taylor-Hood finite element space,

$$p^h = \mathbf{N}_p \mathbf{P} \tag{14a}$$

$$T^h = \mathbf{N}_T \mathbf{T} \tag{14b}$$

$$\mathbf{u}^h = \mathbf{N}_u \mathbf{U} \tag{14c}$$

where $\mathbf{P}$, $\mathbf{T}$, $\mathbf{U}$ are the vectors of the nodal values of the unknowns. $\mathbf{N}_p$, $\mathbf{N}_T$, $\mathbf{N}_u$ are the shape functions respectively. Achieving a reasonable numerical stability and accuracy requires the use of linear interpolation functions for pressure and temperature variables and quadratic interpolation functions for displacement variables (Korsawe et al., 2006).

As we assume continuity of pressure and temperature over the two systems, i.e. porous media and discrete fractures, ($p^m = p^f$, $T^m = T^f \quad \forall \mathbf{x} \in \Gamma_d$), and have elements for the both systems sharing the same nodes, the nodal vector of pressure and temperature for the fractures becomes a subset of those for porous media. Therefore, after discretization in space, weak forms for two distinct systems can be superimposed. In addition, by superimposing the flux contributions at each node from both element types, the terms for flux exchange between the two systems (q^+, q^-) balance off and its explicit calculation is unnecessary (Woodbury and Zhang, 2001; Segura and Carol, 2004).

Finally, finite element formulations of the governing equations can be written in a matrix form as

Hydraulic process

$$\mathbf{M}_H^m \dot{\mathbf{P}}^m + \mathbf{K}_H^m \mathbf{P}^m + \mathbf{C}^{mT} \dot{\mathbf{U}} - \mathbf{f}_H^m = 0 \tag{15a}$$

$$\mathbf{M}_H^f \dot{\mathbf{P}}^f + \mathbf{K}_H^f \mathbf{P}^f + \mathbf{C}^{f^T} [\![\dot{\mathbf{U}}]\!] - \mathbf{f}_H^f = 0 \tag{15b}$$

Heat transport process

$$\mathbf{M}_T^m \dot{\mathbf{T}}^m + \mathbf{K}_T^m \mathbf{T}^m - \mathbf{f}_T^m = 0 \tag{15c}$$

$$\mathbf{M}_T^f \dot{\mathbf{T}}^f + \mathbf{K}_T^f \mathbf{T}^f - \mathbf{f}_T^f = 0 \tag{15d}$$

Mechanical process

$$\int_\Omega \mathbf{B}^T \boldsymbol{\sigma}' \, \mathrm{d}\Omega - \mathbf{C}^m \mathbf{P}^m + \int_{\Gamma_d} \mathbf{N}_u^{f^T} \mathbf{t}_d'^- \, \mathrm{d}\Gamma - \mathbf{C}^f \mathbf{P}^f - \mathbf{f}_M = 0 \tag{15e}$$

where $\mathbf{P}$, $\mathbf{T}$ and $\mathbf{U}$ are the primary node variables of fluid pressure, temperature and displacements. $\mathbf{M}$, $\mathbf{K}$ and $\mathbf{C}$ are process-specific mass, Laplace and coupling matrices. $\mathbf{f}$

is the right-hand-side term contained the contributions of the coupled processes. $\mathbf{B}$ is the strain-displacement matrix. Details of the process-specific matrices are as follows:

$$\mathbf{M}_H^m = \int_\Omega \mathbf{N}_p^{m^T} S_s \mathbf{N}_p^m \, \mathrm{d}\Omega \tag{16a}$$

$$\mathbf{K}_H^m = \int_\Omega \nabla \mathbf{N}_p^{m^T} \frac{\mathbf{k}}{\mu} \nabla \mathbf{N}_p^m \, \mathrm{d}\Omega \tag{16b}$$

$$\mathbf{f}_H^m = -\mathbf{K}_H^m \rho^l \mathbf{g} - \int_{\Gamma_q} \mathbf{N}_p^{m^T} \bar{q} \, \mathrm{d}\Gamma \tag{16c}$$

$$\mathbf{M}_H^f = \int_{\Gamma_\mathrm{d}} b_m \mathbf{N}_p^{f^T} S_s \mathbf{N}_p^f \, \mathrm{d}\Gamma \tag{16d}$$

$$\mathbf{K}_H^f = \int_{\Gamma_\mathrm{d}} \nabla \mathbf{N}_p^{f^T} (b_h \frac{\mathbf{k}}{\mu} \nabla \mathbf{N}_p^f) \, \mathrm{d}\Gamma \tag{16e}$$

$$\mathbf{f}_H^f = -\mathbf{K}_H^f \rho^l \mathbf{g} - \int_{\Gamma_q} \mathbf{N}_p^{f^T} \bar{q} \, \mathrm{d}\Gamma \tag{16f}$$

$$\mathbf{C}^m = \int_\Omega \mathbf{B}^T \alpha \mathbf{m}^m \mathbf{N}_p^m \, \mathrm{d}\Omega \tag{16g}$$

$$\mathbf{C}^f = \int_{\Gamma_\mathrm{d}} \mathbf{N}_u^{f^T} \alpha \mathbf{R}^T \mathbf{m}^f \mathbf{N}_p^f \, \mathrm{d}\Gamma \tag{16h}$$

$$\mathbf{M}_T^m = \int_\Omega \mathbf{N}_T^{m^T} c_p \rho \mathbf{N}_T^m \, \mathrm{d}\Omega \tag{16i}$$

$$\mathbf{K}_T^m = \int_\Omega \mathbf{N}_T^\mathrm{T} c_p^l \rho^l \mathbf{q}_H \cdot \nabla \mathbf{N}_T \, \mathrm{d}\Omega + \int_\Omega \nabla \mathbf{N}_T^\mathrm{T} \lambda \nabla \mathbf{N}_T \, \mathrm{d}\Omega \tag{16j}$$

$$\mathbf{f}_T^m = \int_\Gamma \mathbf{N}_T^\mathrm{T} \mathbf{q}_T \cdot \mathbf{n} \, \mathrm{d}\Gamma + \int_\Omega \mathbf{N}_T^\mathrm{T} Q_T \, \mathrm{d}\Omega \tag{16k}$$

$$\mathbf{M}_T^f = \int_{\Gamma_\mathrm{d}} \mathbf{N}_T^{f^T} c_p^l \rho^l \mathbf{N}_T^f \, \mathrm{d}\Gamma \tag{16l}$$

$$\mathbf{K}_T^f = \int_{\Gamma_\mathrm{d}} \mathbf{N}_T^\mathrm{T} b_h c_p^l \rho^l \mathbf{q}_H \cdot \nabla \mathbf{N}_T \, \mathrm{d}\Gamma + \int_\Omega \nabla \mathbf{N}_T^\mathrm{T} b_m \lambda^l \nabla \mathbf{N}_T \, \mathrm{d}\Omega \tag{16m}$$

$$\mathbf{f}_T^m = \int_\Gamma \mathbf{N}_T^\mathrm{T} \mathbf{q}_T \cdot \mathbf{n} \, \mathrm{d}\Gamma + \int_{\Gamma_\mathrm{d}} \mathbf{N}_T^\mathrm{T} Q_T \, \mathrm{d}\Gamma \tag{16n}$$

$$\mathbf{f}_M = \int_\Omega \mathbf{N}_u^{m^T} \rho \mathbf{g} \, \mathrm{d}\Omega + \int_{\Gamma_t} \mathbf{N}_u^{m^T} \bar{\mathbf{t}} \, \mathrm{d}\Gamma \tag{16o}$$

$$\tag{16p}$$

with $\mathbf{m}$ a mapping vector as $\mathbf{m}^m = (1, 1, 1, 0)$, $\mathbf{m}^f = (0, 1) \; \forall \mathbf{x} \in \mathbb{R}^\mathbf{2}$ and $\mathbf{m}^m = (1, 1, 1, 0, 0, 0)$, $\mathbf{m}^f = (0, 0, 1) \; \forall \mathbf{x} \in \mathbb{R}^\mathbf{3}$. $\mathbf{D}$ is the elastic constitutive tensor.

We keep $\boldsymbol{\sigma}'$, $\mathbf{t}_\mathrm{d}'^-$ in the equation (15e) in order to easily rewrite the equations into an incremental form and also for, which is adequate for the nonlinear analysis. Incremental form of the integration terms for $\boldsymbol{\sigma}'$ and $\mathbf{t}_\mathrm{d}'^-$ appeared in equation (15e) can be formulated with nodal unknowns $\mathbf{U}$ and $[\![\mathbf{U}]\!]$ as,

$$\int_\Omega \mathbf{B}^T \Delta \boldsymbol{\sigma}' \, \mathrm{d}\Omega = \int_\Omega \mathbf{B}^T \mathbf{D}_e \mathbf{B} \, \mathrm{d}\Omega \, \Delta \mathbf{U} \tag{17a}$$

$$\int_{\Gamma d} \mathbf{N}_u^{fT} \Delta \mathbf{t}_d'^- \, d\Gamma = \int_{\Gamma d} \mathbf{N}_u^{fT} \mathbf{R}^T \mathbf{K} \mathbf{R} \mathbf{N}_u^f \, d\Gamma \, \Delta [\![\mathbf{U}]\!] \tag{17b}$$

where $\mathbf{D}_e$ is the elastic material tensor.

Time discretization to approximate the solutions of the ordinary differential equations (15a), (15b), (15c) and (15d) is accomplished through the first order finite difference scheme. The momentum balance equation is considered as a quasi-static problem.

3.5 Coordinate transformation for discrete fracture elements

Discrete fractures can be represented by lower-dimensional elements, e.g. 1-D elements in $\mathbb{R}^2$ and 2-D elements in $\mathbb{R}^3$. The elements are mapped into $\mathbb{R}^1$ and $\mathbb{R}^2$, respectively. Integrations for discrete fracture space require coordinate transformation.

Coordinate transformation   Consider that $\mathbf{x}$ is a directional vector in global coordinates (x-y-z), and $\mathbf{x}'$ is that in local coordinates (x'-y'). Coordinate transformation between the two coordinates can be achieved with a rotational matrix $\mathbf{R}$ as

$$\mathbf{x} = \mathbf{R}\mathbf{x}'. \tag{18}$$

In two-dimensional space, the rotational matrix is

$$\mathbf{R}_{2D} = \begin{bmatrix} \cos\theta & -\sin\theta \\ \sin\theta & \cos\theta \end{bmatrix} \tag{19}$$

with a rotational angle θ between x and x'. The cosine and sine functions can be simply calculated by the following formulas:

$$\cos\theta = \frac{v_x}{|\mathbf{v}|}, \qquad \sin\theta = \frac{v_y}{|\mathbf{v}|} \tag{20}$$

where $\mathbf{v}$ is a vector aligning with x'. In three-dimensional space, the rotation matrix is given as

$$\mathbf{R}_{3D} = \begin{bmatrix} \cos(x',x) & \cos(x',y) & \cos(x',z) \\ \cos(y',x) & \cos(y',y) & \cos(y',z) \\ \cos(z',x) & \cos(z',y) & \cos(z',z) \end{bmatrix} \tag{21}$$

with the directional cosines $\cos(x_i', x_j)$, which is a cosine of angle between the axes x_i' and x_j. A directional cosine is calculated as

$$\cos(\mathbf{v}, \mathbf{x}) = \frac{\mathbf{v} \cdot \mathbf{x}}{|\mathbf{v}|} \tag{22}$$

for a vector $\mathbf{v}$ and a unit vector $\mathbf{x}$. The vector $\mathbf{x}'$ can be given by

$$\mathbf{x}' = \mathbf{x}_1 - \mathbf{x}_0 \tag{23}$$
$$\mathbf{y}' = \mathbf{z}' \times \mathbf{x}' \tag{24}$$
$$\mathbf{z}' = \mathbf{x}' \times (\mathbf{x}_2 - \mathbf{x}_1) \tag{25}$$

Directional material parameters Directional material parameters, e.g. permeability tensor $\mathbf{k}$, have to be evaluated in appropriate coordinate systems. A parameter in local coordinates $\mathbf{k}'$ can be transformed into the one in global coordinates $\mathbf{k}$ as:

$$\mathbf{k} = \mathbf{R}\mathbf{k}'\mathbf{R}^T \tag{26}$$

Shape functions Coordinate transformation of directional shape functions associated with vector variables $\mathbf{u} = \{u_x, u_y, u_z\}^T$ is given by

$$\mathbf{u}_e^h(x,y,z) = \mathbf{R}\mathbf{u}_e'^h(x',y') = \sum_i \left[\mathbf{R}\mathbf{N}_i(r,s)\mathbf{u}_i'\right] = \sum_i \left[\mathbf{R}\mathbf{N}_i(r,s)\mathbf{R}^T\mathbf{u}_i\right] \tag{27}$$

where i is an elemental node index.

Derivatives of shape functions Derivatives of scalar shape functions are given by

$$\nabla N(x,y,z) = \mathbf{J}_{x-x'}^{-1}\nabla N(x',y') = \mathbf{J}_{x-x'}^{-1}\left(\mathbf{J}_{x'-r}^{-1}\nabla N(r,s)\right) = \mathbf{R}^T\left(\mathbf{J}_{x'-r}^{-1}\nabla N(r,s)\right) \tag{28}$$

Assuming a perfectly flat plane, $\mathbf{J}_{x-x'}^{-1}$ can be replaced by $\mathbf{R}$. Derivatives of directional (vector) shape functions are

$$\nabla\mathbf{N}(x,y,z) = \nabla\left[\mathbf{R}\mathbf{N}(x',y')\mathbf{R}^T\right] = \mathbf{R}\left[\mathbf{J}_{x'-r}^{-1}\nabla\mathbf{N}(r,s)\right]\mathbf{R}^T \tag{29}$$

Example in evaluating a conductive matrix An example of the coordinate transformation is explained for a directional permeability tensor in the volume balance equation for discrete fractures. The fracture permeability is usually given in its local coordinate systems. Thus the information has to be transformed into global coordinates to evaluate the equation.

Consider a line element e representing a fracture in 2-D spaces. The element is placed on a perfectly flat plane. It is known that the fracture has a permeability tensor $\mathbf{k}'$ defined in local coordinate systems which can be transformed into global coordinates with a rotation matrix R_f. To evaluate a conductive matrix $\mathbf{K}$ in the balance equation, local coordinates have to be transformed into global coordinates. Conductive matrix $\mathbf{K}_e^f$ can be formulated in natural coordinate systems as

$$\mathbf{K}_e^f = \int_{\Gamma^e} b_h \nabla\mathbf{N}(\mathbf{x})^T \frac{\mathbf{k}}{\mu} \nabla\mathbf{N}(\mathbf{x})d\Gamma \tag{30}$$

$$= \int_{-1}^{+1} b_h \left(\mathbf{R}_e^T\mathbf{J}^{-1}\nabla\mathbf{N}(\mathbf{r})\right)^T \frac{\mathbf{R}_f\mathbf{k}'\mathbf{R}_f^T}{\mu} \left(\mathbf{R}_e^T\mathbf{J}^{-1}\nabla\mathbf{N}(\mathbf{r})\right) \det\mathbf{J}dr \tag{31}$$

where $\mathbf{R}_e$ is a rotation matrix for elements and $\mathbf{J}$ is the Jacobian matrix transferring the physical coordinates to the natural coordinates.

3.6 Approximation of geomechanical discontinuities

3.6.1 Introduction

From a mathematical standpoint, discrete fractures are considered as mechanical discontinuities. The fracture acts as an interface between rock blocks, where displacements at the edge of one block are not identical to the other side. This makes it difficult to solve the problem using continuity based numerical methods such as the FEM (Jing, 2003).

Major approaches to include the discontinuities within the FEM can be the followings:

- Interface elements approach

- Enrichment approach: generalized/extended FEM

The FEM with interface elements (IEs) is a widely used approach for geotechnical engineering. Essentially, this approach approximates a discontinuous function with a continuous function by representing a fracture as a solid entity with/without thickness. The approach was first proposed as zero-thickness elements or Goodmans's joint elements (Goodman et al., 1968) and has attracted attention because of its simplicity to implement into conventional FEM (Jing, 2003). The IEs have also been utilized for coupled HM or THM problems with pre-existing fractures (Guvanasen and Chan, 2000; Noorishad et al., 1992; Ng and Small, 1997).

An additional approach utilized to represent fractures is an enrichment approximation such as the extended finite element method (XFEM) developed for a crack analysis (Belytschko and Black, 1999; Moës et al., 1999). One can find a comprehensive review of the method in the literature (Abdelaziz and Hamouine, 2008; Fries and Belytschko, 2010). The XFEM handles discontinuities directly in an approximation space with jump functions, i.e. local enrichment functions, and consequently there is no need to represent them in a mesh. This significantly reduces the cost of re-meshing for crack growth, which is required in a conventional FEM. Disadvantages include higher computational cost due to a variable number of degrees of freedom and greater complexity in numerical integration, such as subdivision of elements.

Both approaches may start with the following assumptions: (1) Effect of fractures appears in the relationship of boundary forces of two intact rocks. (2) Fractures behave as spring systems which make a link between two intact rocks.

In the following, zero-thickness interface elements and lower-dimensional interface elements with local enrichments [EP2] are presented for an example illustrated in Figure 4. The domain Ω is bounded by a boundary Γ and includes a discontinuity Γ_d. The domain can be subdivided into Ω^+ and Ω^- along the discontinuity plane. The normal vector $\mathbf{n}_\mathrm{d}^+$ indicates the direction of Ω^+ from the discontinuity plane. The displacement function $\mathbf{u}(\mathbf{x})$ is strongly discontinuous at the discontinuity plane Γ_d (Figure 6).

3.6.2 Zero-thickness interface elements

Goodman et al. (1968) has proposed zero thickness joint elements to model mechanical behavior of rocks including a specific discontinuity. The model does not explicitly have a fracture aperture in a numerical mesh, but it is represented as relative displacements. Interpolation function assumes values are same along y' axis and are vary along x' axis. Although the Goodman's joint element is originally 4-nodes linear element, it can be extended to 6-nodes quadratic elements which correspond to quadratic elements used for intact rocks (Figure 5).
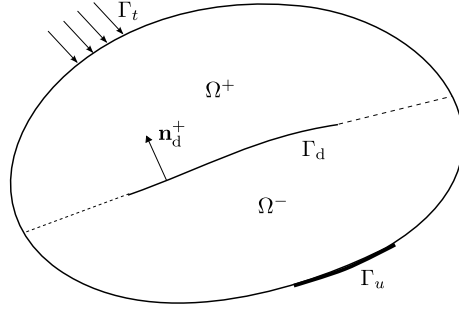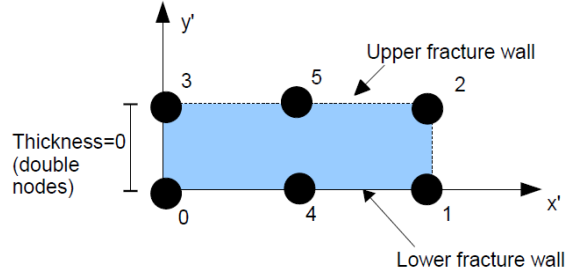
Figure 4: Domain with a discontinuity

Figure 5: Zero-thickness interface elements in 2D, quadratic

Relative displacement   Relative displacements $\mathbf{w}$ are given by difference between solid displacements $\mathbf{u}$ at upper $(+)$ and lower $(-)$ surfaces:

$$
\begin{aligned}
\mathbf{w} &= \left\{ \begin{array}{c} u_{\mathrm{n}}^{+} - u_{\mathrm{n}}^{-} \\ u_{\mathrm{s}}^{+} - u_{\mathrm{s}}^{-} \end{array} \right\} = \begin{bmatrix} -1 & 1 & 0 & 0 \\ 0 & 0 & -1 & 1 \end{bmatrix} \left\{ \begin{array}{c} u_{\mathrm{n}}^{-} \\ u_{\mathrm{n}}^{+} \\ u_{\mathrm{s}}^{-} \\ u_{\mathrm{s}}^{+} \end{array} \right\} \\[2mm]
&= \mathbf{LHu}' = \mathbf{RLHu}
\end{aligned}
\tag{32}
$$

where $\mathbf{u}'$ is a nodal vector of displacement in local coordinates given as

$$
\mathbf{u}' = \left\{ u_1'\, u_2'\, \ldots\, u_6'\, v_1'\, v_2'\, \ldots\, v_6' \right\}^{T}
\tag{33}
$$

and $\mathbf{R}$ is a rotational matrix. $\mathbf{L}$ and $\mathbf{H}$ are defined as

$$
\mathbf{L} = \begin{bmatrix} -1 & 1 & 0 & 0 \\ 0 & 0 & -1 & 1 \end{bmatrix}, \ \mathbf{H} = \begin{bmatrix} \mathbf{N} & 0 & 0 & 0 \\ 0 & \mathbf{N} & 0 & 0 \\ 0 & 0 & \mathbf{N} & 0 \\ 0 & 0 & 0 & \mathbf{N} \end{bmatrix}
\tag{34}
$$

with a shape function vector for quadratic line elements $\mathbf{N}$.

Effective stress vector   Internal effective stress vector in the fracture $\boldsymbol{\sigma}'^{f}$ can be expressed as

$$
d\boldsymbol{\sigma}'^{f} = \mathbf{K}d\mathbf{w} = \mathbf{KRLH}\,d\mathbf{u}
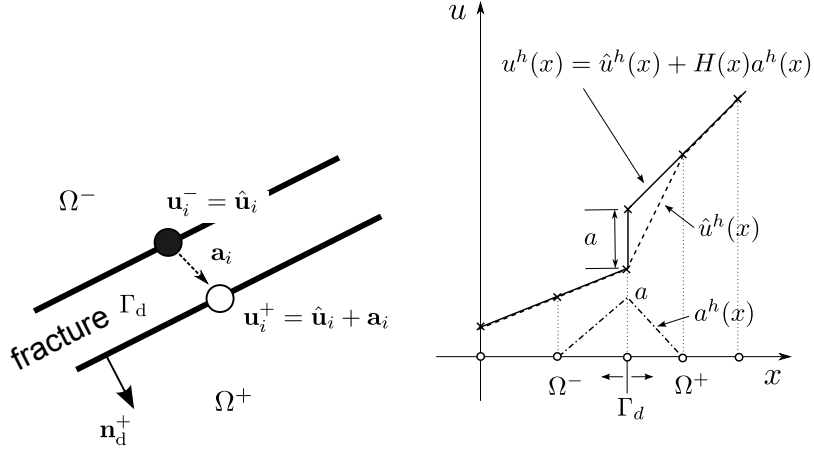\tag{35}
$$

20

Figure 6: Single discontinuity (left) and the approximated displacement field with jump (right)

with the joint stiffness matrix $\mathbf{K}$. It leads for the integration form to

$$\int_{\Gamma_d} [\![\boldsymbol{\omega}]\!]^T d\boldsymbol{\sigma}'^f \, \mathrm{d}\Gamma = \int_{\Gamma_d} (\mathbf{RLH}\boldsymbol{\omega})^T d\boldsymbol{\sigma}'^f \, \mathrm{d}\Gamma = \int_{\Gamma_d} (\mathbf{RLH}\boldsymbol{\omega})^T \mathbf{KRLH} \, \mathrm{d}\Gamma \, d\mathbf{u} \, . \qquad (36)$$

3.6.3 Lower-dimensional interface elements with local enrichments

Watanabe et al. (2011) has developed lower-dimensional interface elements (LIEs) with local enrichments [EP2]. The method represents the displacement function $\mathbf{u}(\mathbf{x})$ with local enrichments. To express the discontinuous function $\mathbf{u}(\mathbf{x})$ using continuous functions, a function $\mathbf{a}(\mathbf{x}) \in \mathcal{V} \in H_0^1(\Omega)$ is introduced with a finite dimensional space $\mathcal{V}$, and the function is called a *displacement jump* function. The function is defined as

$$\mathbf{a}(\mathbf{x}) = \begin{cases} \mathbf{u}^+(\mathbf{x}) - \mathbf{u}^-(\mathbf{x}) & \text{if } \mathbf{x} \text{ is on } \Gamma_d \\ & \text{and not on the edges of } \Gamma_d \\ 0 & \text{else} \end{cases} \qquad (37)$$

where $\mathbf{a}(\mathbf{x})$ implies the displacement jump on the discontinuity plane Γ_d. We then introduce another function $\hat{\mathbf{u}}(\mathbf{x}) \in \mathcal{V}$, called a *regular displacement* function with a definition, $\hat{\mathbf{u}} = \mathbf{u}^-$ on Γ_d^-. Hence the displacement function can be expressed with the two functions as below.

$$\mathbf{u}(\mathbf{x}) = \begin{cases} \hat{\mathbf{u}}(\mathbf{x}) + \mathbf{a}(\mathbf{x}) & \text{if } \mathbf{x} \text{ is on } \Gamma_d^+ \\ \hat{\mathbf{u}}(\mathbf{x}) & \text{else} \end{cases} \qquad (38)$$

An example of the discontinuous displacement function is illustrated in Figure 6. As shown in Figure 6 (left), the displacement at node i on the side of the domain Ω^+, which is expressed as $\mathbf{u}_i^+$, is defined by superposition of $\hat{\mathbf{u}}_i$ and $\mathbf{a}_i$. On the other side, $\mathbf{u}_i^-$ is defined only by $\hat{\mathbf{u}}_i$. While Figure 6 (right) depicts the displacement function within the threshold of the discontinuity.

Using the above definitions, we approximate the displacement function $\mathbf{u}(\mathbf{x})$ by using

21

local enrichments. The FE approximation is given as

$$\mathbf{u}^h(\mathbf{x}) = \sum_{i \in I} N_i^m(\mathbf{x})\hat{\mathbf{u}}_i + \sum_{i \in I_d} N_i^m(\mathbf{x})\psi_d(\mathbf{x})\,\mathbf{a}_i \tag{39}$$

where the first term corresponds to the standard FE approximation with the regular displacement $\hat{\mathbf{u}}_i$, and the second term corresponds to the local enrichment approximation with the jump function $\mathbf{a}_i$. I is the set of all nodes in the domain, $N_i^m(\mathbf{x}) \in \mathcal{V}$ is a shape function for porous media at node i, I_d is a nodal subset of the enrichment on the discontinuity Γ_d, and $\psi_d(\mathbf{x})$ is a global enrichment function. For strong discontinuity problems, the global enrichment function can be described by the Heaviside step function as

$$\psi_d(\mathbf{x}) = H(f_d(\mathbf{x})) = \begin{cases} 1 & \text{for } x \in \Omega^+ \\ 0 & \text{for } x \in \Omega^- \end{cases} \tag{40}$$

with the Level-set function $f_d(\mathbf{x})$ implicitly representing the discontinuity plane. The function $f_d(\mathbf{x})$ is, in this case, a signed distance function giving positive if $\mathbf{x}$ is in a region Ω^+, and negative in Ω^-.

Relative displacement The fracture relative displacement in global coordinates $\llbracket\mathbf{u}\rrbracket(\mathbf{x})$ can be defined with the displacement jump function $\mathbf{a}(\mathbf{x})$. As shown in Figure 6, for a single discontinuity, the jump function is identical to the fracture relative displacement,

$$\llbracket\mathbf{u}\rrbracket = \mathbf{a}. \tag{41}$$

A FE approximation of the fracture relative displacement function $\llbracket\mathbf{u}\rrbracket(\mathbf{x})$ is in a standard FEM manner from the equation (41). The approximation is given as,

$$\llbracket\mathbf{u}\rrbracket^h(\mathbf{x}) = \sum_{i \in I_d} N_i^f(\mathbf{x})\,\mathbf{a}_i \tag{42}$$

where I_d is the set of all nodes on the discontinuity Γ_d, $N_i^f(\mathbf{x})$ is a shape function for discrete fractures at node i, which satisfies $N_i^f(\mathbf{x}) \in \mathcal{V}$, $N_i^f(\mathbf{x}) \in N_i^m(\mathbf{x})$ for consistency of $\llbracket\mathbf{u}\rrbracket^h(\mathbf{x})$ in equation (39) and (42).

Effective stress vector Internal effective stress vector in the fracture $\boldsymbol{\sigma}'^f$ can be expressed as

$$d\boldsymbol{\sigma}'^f = \mathbf{K}d\mathbf{w} = \mathbf{K}\mathbf{R}\mathbf{N}d\llbracket\mathbf{u}\rrbracket. \tag{43}$$

It leads for the integration form to

$$\int_{\Gamma_d} \llbracket\boldsymbol{\omega}\rrbracket^T d\boldsymbol{\sigma}'^f \, d\Gamma = \int_{\Gamma_d} (\mathbf{R}\mathbf{N}\delta\mathbf{a})^T d\boldsymbol{\sigma}'^f \, d\Gamma = \int_{\Gamma_d} (\mathbf{R}\mathbf{N}\delta\mathbf{a})^T \mathbf{K}\mathbf{R}\mathbf{N} \, d\Gamma \, d\mathbf{a}. \tag{44}$$

3.7 Solution procedures and computational efficiency

3.7.1 Coupling strategy for T-H-M

Coupling strategy for the coupled THM problems has to be chosen depending on strength of coupling between processes: (1) fully monolithic, (2) partly partitioned, and (3) fully partitioned. If all processes strongly couple each other, fully monolithic method, i.e. solving

all three equations in a simultaneous equation, would be appropriate. The second approach is for a case that coupling between two equations is much stronger than that with the rest one. Fully partitioned approach can be applied when all equations are weakly coupled.

For non-isothermal single phase flow in deformable porous media, partitioned approach can be applied for simulating the long-term behavior. As far as time step size is enough large, HM coupling effects are not strong. If fracture aperture change is allowed, HM processes become a strong coupling problem. Thermal coupling effects in those two processes are less significant. Thus one can partition the equations to HM and T, and solve the two equations individually.

3.7.2 Parallelization

In the finite element (FE) analysis of coupled THM problems, computation time depends mainly on number of field variables and coupling among processes. The number of field variables is related with a mesh size and solved physical processes, i.e. number of matrices and size of each matrix to be solved. Because coupling among the process is made in an iterative way, more coupling iteration count means more computation time because it requires recalculation of all processes each time.

The parallelization method is based upon the domain decomposition concept in order to split the topological discretization of whole model domain (i.e. finite element mesh) into several sub-domains. Then the finite element contributions are assembled for each of those sub-domains. Finally the sub-domain contributions are reconciled to obtain a solution of the original problem for the whole domain. In general, the parallelization concept consists of following three basic steps: (1) domain decomposition, (2) partitioning of global assembly of the algebraic equation systems; i.e. assembly of local sub-domain matrices and vectors of each T-H-M process, and (3) partitioning of the global linear solver. We consider geometric parallelism, which means that all CPU nodes of a parallel machine run the same code for the existing domain decomposition. Message Passing Interface (MPI) is used to make parallel computation. The domain is decomposed with excellent software METIS (Karypis and Kumar, 1998). The parallel finite element method for THM coupled problems is in detail described by Wang et al. (2009).
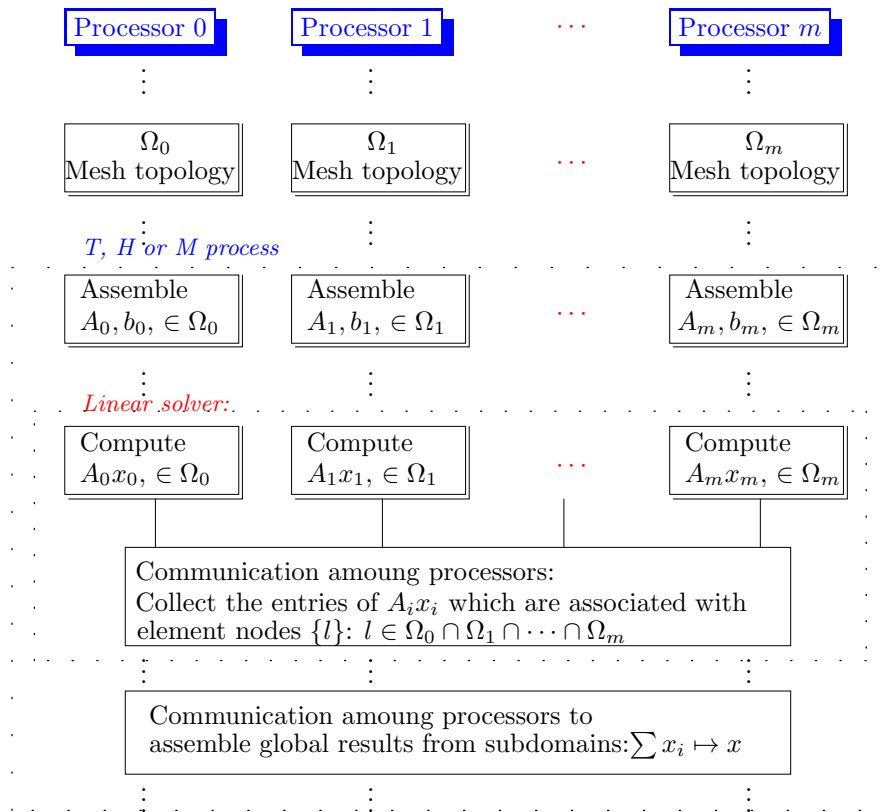
Figure 7: Schematic of the parallel finite element method (Wang et al., 2009)

4 Examples and Applications

4.1 Selected verification examples

4.1.1 Example 1: 2D groundwater flow problem

This example is presented to validate the hybrid model of discrete fractures and porous media for modeling groundwater flow. Consider a 2D infinite horizontal plane of porous media with an embedded fracture at the center of the domain. Uniform flow with specific discharge q_0 occurs from the left side to the right of the domain. The fracture geometry is illustrated in Figure 8. The fracture has a length of L and is inclined with angle α. The fracture aperture b may vary with positions. In this example, it is assumed that the shape corresponds to that obtained from the normal displacements of the sides of a pressurized crack in an elastic medium. This gives $b = b_{\max}\sqrt{1 - x'^2}$ where x' is the normalized local coordinate systems. $b_{\max}$ is the aperture at the cen-

Figure 8: Fracture geometry

ter $x' = 0$. Assuming the volume of the fracture is sufficiently small as compared to that of porous media, the flow in the porous media can be modeled ignoring the width of the fracture. The flow in the fracture is assumed to be laminar along the fracture surface. Hydraulic conductivity of the fracture is constant and independent of the aperture variation. The pressure variation across the fracture is neglected.
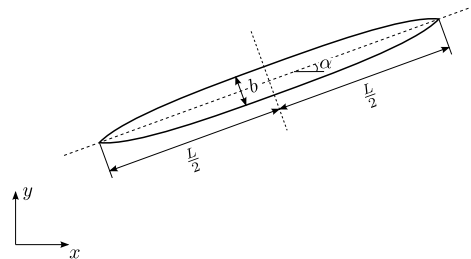
Table 2: Model parameters

Parameter	
Fracture angle	45 °
Maximum fracture aperture	0.05 m
Fracture length	2.0 m
Fracture hydraulic conductivity	1.0×10^{-3} m/s
Porous medium hydraulic conductivity	1.0×10^{-5} m/s
Specific discharge	1.0×10^{-4} m/s

Numerical solution for this problem can be obtained by solving the steady state liquid flow equation with a hybrid model of a discrete fracture and porous media. The fracture is represented as a 1D hydraulic conduit. The domain is set up in a finite space as a square with length of 10 m as depicted in Figure 9. To compare numerical results in a finite domain with an analytical solution (Strack, 1982) in an infinite domain, pressure calculated by the analytical solution with specific discharge $q_0 = 1.0 \times 10^{-4}$ m/s is utilized as prescribed pressure at the lateral boundaries, i.e. $p_{\text{in}} = 496465$ Pa and $p_{\text{out}} = -496465$ Pa. The numerical model assumes that the fracture aperture does not vary with positions and has constant value even at the endpoints, $b = b_{\max}$.

Pressure distribution obtained by the analytical solution is shown in Figure 10. Lateral uniform flow is disturbed in the vicinity of the inclined fracture where groundwater flows faster than in surrounding porous media. Figure 11 presents the pressure profile along a diagonal line from the bottom-left to the top-right. Although the numerical solution adopts
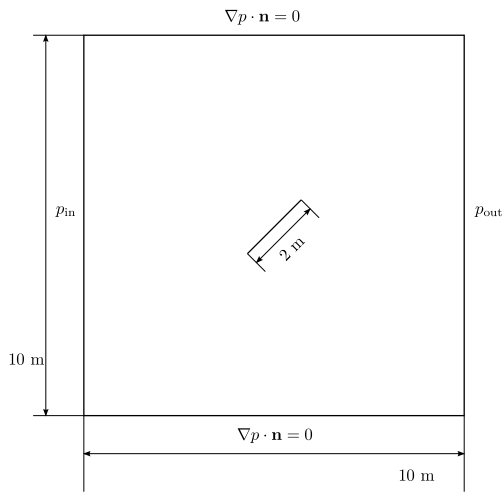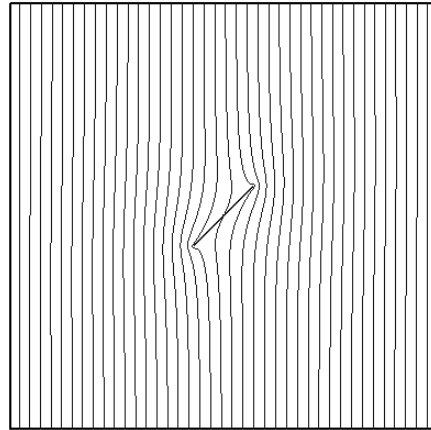
Figure 9: Computational area

Figure 10: Pressure distribution obtained by the analytical solution

the idealized fracture geometry, results show good agreements between the numerical and the analytical solution.
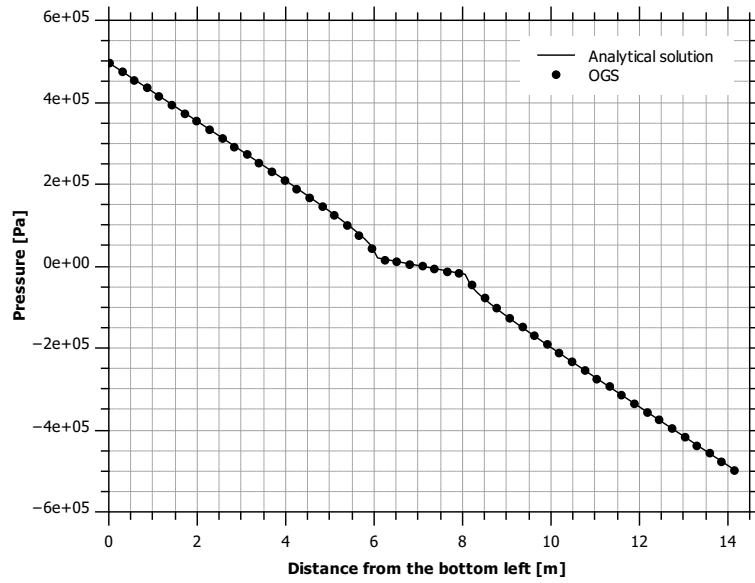

Figure 11: Pressure profile along a diagonal line from the bottom-left to the top-right

4.1.2 Example 2: 2D coupled hydro-mechanical problem

This example illustrates a fluid injection problem into a single discrete fracture surrounded by an impermeable rock matrix in 2D space and validates the proposed lower-dimensional interface elements with local enrichments for the nonlinear, coupled HM problem [EP2]. The test case is designed to mimic the semi-analytical similarity solution available in Wijesinghe (1986).

As illustrated in Figure 12, the major fracture lies horizontally in the middle of an impermeable rock block. The fracture is subjected to a uniform in-situ stress σ_{yy} normal to the fracture. Initially, fracture aperture is uniformly $b_0 = 1.0 \times 10^{-2}$ mm and fluid pressure is $p_0 = 11.0$ MPa along the fracture. At time $t = 0^+$, fluid is injected at the left-most edge of the fracture (in the form of constant boundary pressure, $p = 11.9$ MPa) and a sudden increase of pressure in the fracture results. The injection pressure induces elastic fracture opening and a subsequent increase of fracture permeability and storage capacity. Stress in the surrounding rocks is 50 MPa and fluid pressure is 11 MPa. Boundary fluid pressure is fixed at $t = 0^+$ to 11.9 MPa at the left and 11 MPa at the right. Line elements were used to represent the discrete fracture and quadrilateral elements for surrounding rock matrix. Very fine vertical discretization is required near the fracture, i.e. Δy=0.001 m. The time step is selected as 10 s and a Newton-Raphson iteration is utilized to solve the nonlinear equation.
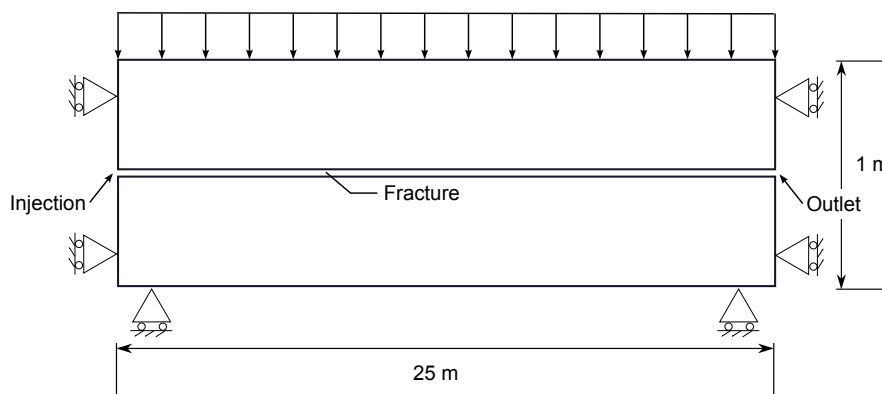

Figure 12: Fluid injection into a discrete fracture-rock matrix system

Simulation results are presented in Figure 13 for pressure and fracture aperture profile along the fracture. When fluid is injected, the fracture aperture is instantaneously opened to nearly 1.9 $\times 10^{-2}$ mm at the injection point ($x = 0$ m). With time, this fracture opening behavior gradually propagates toward the right-most, low-pressure edge of the fracture. Linear constitutive laws dictate a linear variation in fracture aperture relative to fluid pressure. Figure 13 shows, as in all previous examples, strong agreement between the proposed numerical method and the semi-analytical solution.

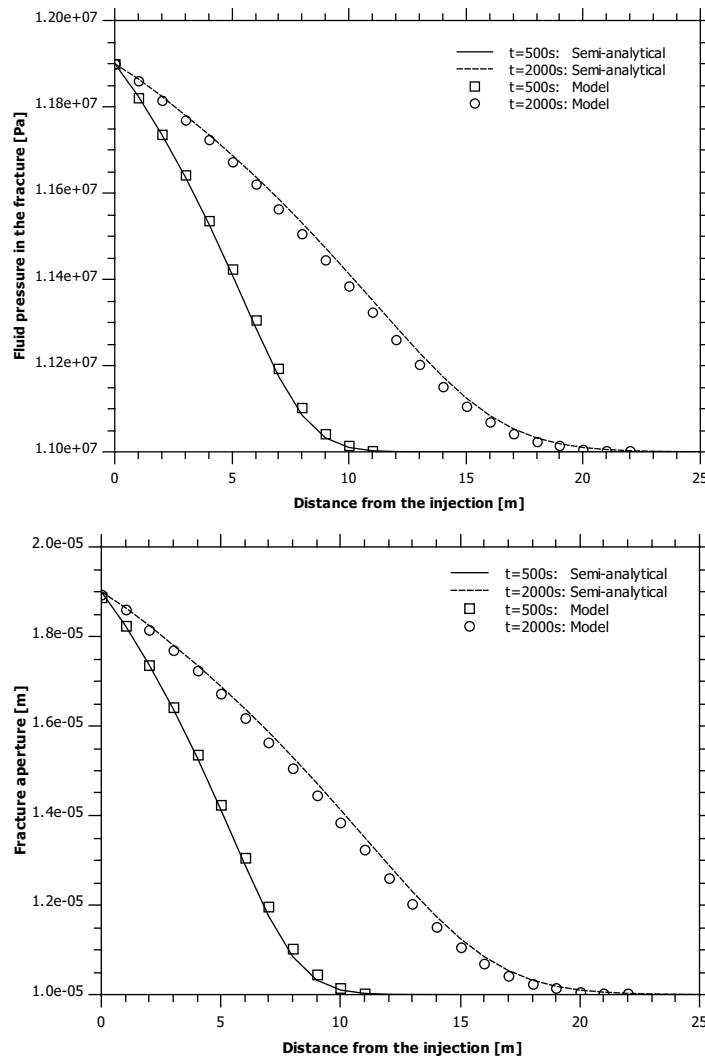| Fluid		Rock (porous medium)	
Density	1000.0 kg/m^3	Density	2716.0 kg/m^3
Viscosity	0.001 Pa s	Specific storage	1.0×10^{-10} Pa^{-1}
		Permeability	1.0×10^{-21} m^2/s
Fracture		Porosity	0.1 %
Initial aperture	1.0×10^{-5} m	Young's modulus	60 GPa
Specific storage	0.0 Pa^{-1}	Poisson ratio	0.0
Joint normal stiffness	100 GPa/m	Biot constant	1.0
Joint shear stiffness	100 GPa/m		
Biot constant	1.0		

Figure 13: Profile along the fracture: pressure (top) and aperture (bottom)

4.2 Deep geothermal reservoir modeling

Coupled thermo-hydro (TH) or hydrothermal model in discretely fractured porous media is applied to the geothermal research wells Gross Schoenebeck in 40 km north of Berlin, Germany. Geometric layout of the reservoir is simplified in this example to reduce complexity in a numerical analysis. The engineered geothermal reservoir is located in -3850 m to -4258 m depth with the average temperature of 150 °C. It has a borehole doublet and four vertical hydraulic fractures (Figure 14). One fracture with the dimension of 143 m height and 160 m length is connected with the injection well, E GrSk3/90, and the other three with the production well, Gt GrSk4/05. The reservoir has six sub-horizontal geological layers. Rock types are silt- and mudstone, sandstone and volcanic rocks. Sub-layers with sandstones at the depth between -3999 m to -4133 m are thought as more hydraulically active area than others due to higher permeability. The highest in-situ reservoir is found as 4-8 mD in sandstones from the laboratory experiments. The hydraulic fractures are oriented to 18 °azimuth which is perpendicular to minimum horizontal stress. Fracture transmissibility has been known as 1 Dm for all hydraulic fractures so that an aperture is derived as 2.28×10^{-4} m. Fluid injection is assumed to be temperature of 70 °C and with salinity of 265 g/l. For further details about the reservoir information, please refer to Blöcher et al. (2010).
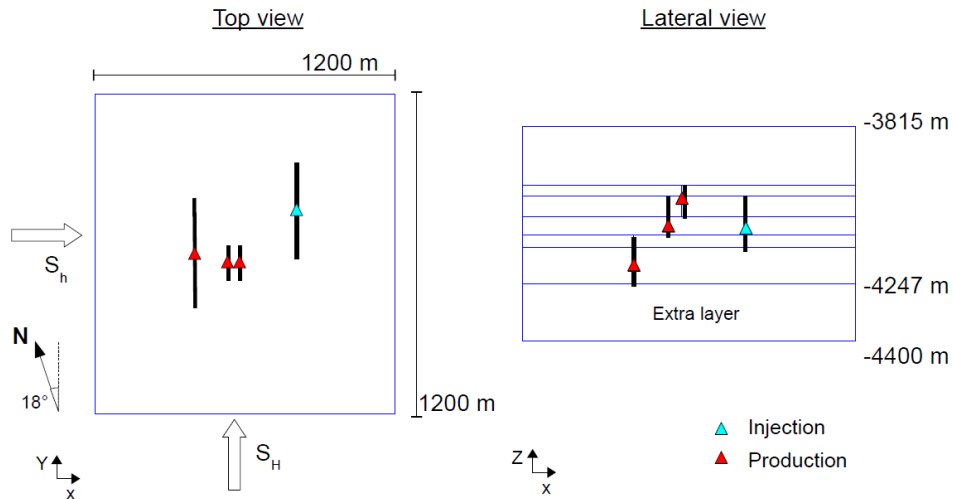

Figure 14: Simplified geometric layout of the Gross Schoenebeck reservoir

In the present model, fluid pressure initially distributes in the range of 41-47 MPa according to a hydrostatic condition. Initial temperature is uniformly 150 °C in the entire domain. It is assumed that the injection well has an overpressure of 5 MPa and the three production wells have an underpressure of 5 MPa. Fluid is injected with temperature of 70°C. Mechanical process is not considered, i.e. only fluid flow and heat transport processes (a coupled TH problem) are taken into account. The fractures are represented with 2D triangle elements and rock matrices are with 3D tetrahedral elements. Material properties used in the simulation are listed in Table 4, 5. Geothermal fluids are non-linear functions of salinity, temperature and pressure (McDermott et al., 2006). To stabilize the numerical oscillations, the SUPG method is used combined with the mass lumping techniques.

Table 4: Rock properties

Unit	Lithology	ρ^s [kg/m^3]	n [%]	$k_x(=4k_z)$ [m^2]	c_p^s [J/kg K]	λ^s [W/m K]	E [GPa]	ν [-]	α_T [1/K]
I	Silt- and mud-stone	2650	1	4.93×10^{-17}	920	1.9			
IIA	Siltstone to fine grained sandstone	2650	3	3.95×10^{-15}	920	1.9	55	0.2	10^{-5}
IIB	Fine grained sandstone	2650	8	1.97×10^{-15}	920	2.9			
IIC	Fine to medium grained sand-stone	2650	15	7.90×10^{-15}	920	2.8			
III	Conglomerates from fine sand-stone to fine grained grave	2650	0.1	9.87×10^{-17}	1000	3.0			
IV	Ryolithe and Andesite	2650	0.5	9.87×10^{-17}	1380	2.3			

Table 5: Hydraulic fracture properties

Well	Type	Unit	b_h [m]	k [m^2]
E GrSk3/90	2 x gel-proppant, 2 x water	IIB, IIC, III	2.28×10^{-4}	4.33×10^{-9}
Gt GrSk4/05	water	III, IV	2.28×10^{-4}	4.33×10^{-9}
	gel-proppant	IIB, IIC	2.28×10^{-4}	4.33×10^{-9}
	gel-proppant	IIA, IIB	2.28×10^{-4}	4.33×10^{-9}

The first results of the coupled TH model in porous media connected to hydraulic fractures represented as discrete fractures are presented. Figure 15 shows the simulated streamline in the reservoir during the fluid circulation. The injected fluid mainly flows in the geological unit IIA, IIB, IIC which has the higher permeability. Flow velocity in porous media is observed in the range of 10^{-3}-10^{-5} m/s. Less fluid flows through the unit III, IV where the permeability is two orders of magnitude less than the unit IIA, IIB, IIC. Because the two outlet fractures close to the inlet fracture are located in the high permeable units, injected fluid mostly flows to those fractures and connected production wells.

In the reservoir, temperature decrease of the rocks is observed due to the cold water injection. After nearly 5 years of the simulation period, the cooling front, i.e. temperature is 1°C below the initial rock temperature, reaches the one of the production wells, which is closest to the injection well (Figure 16). Temperature changes at the three production wells are presented in Figure 17. Temperature drawdown of 10%, which is economically desirable criteria for the geothermal systems (Baria and Petty, 2008), is observed after 14 years at the production well which is the closest to the injection, 17 years at the production well which is the secondly closest to the injection.
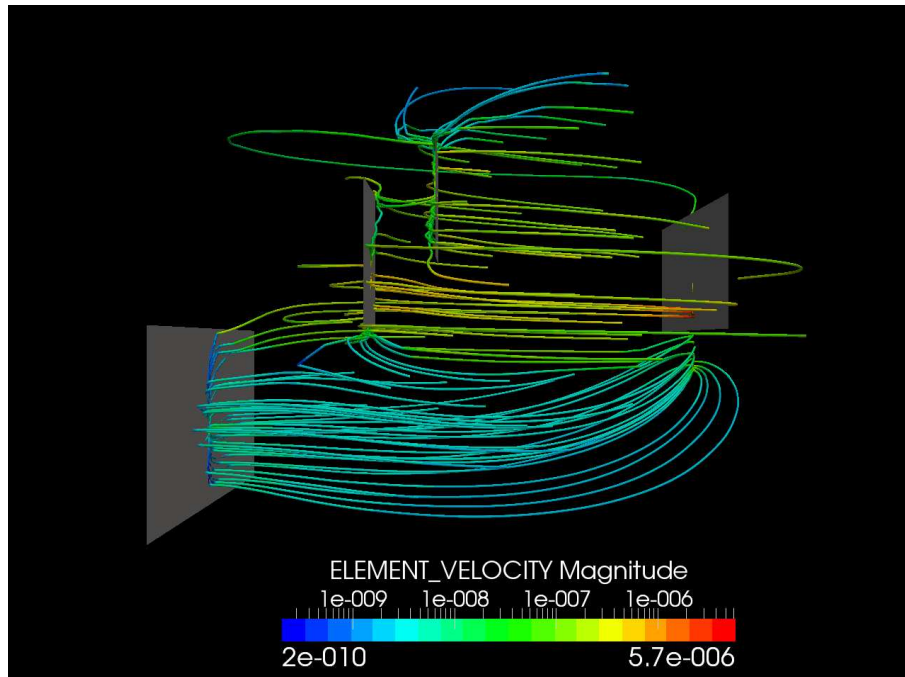
Figure 15: Stream line in the reservoir

This numerical study includes several simplifications, such as geometric layout, uniform initial temperature distribution. Existing fault networks around the reservoir certainly affects the flow system. Couple behavior with mechanical process has to be considered for comprehensive evaluation of the reservoir performance. For instance, Blöcher et al. (2009) have presented impacts of poroelastic response on porosity and permeability in sandstone.
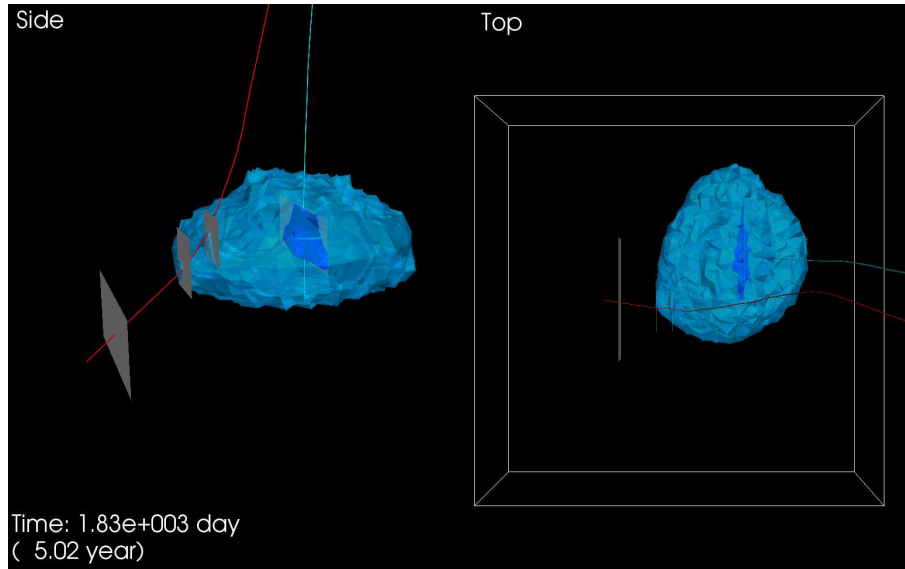
Figure 16: Temperature evolution after injection for nearly 5 years: the light blue iso-surface is 149°C , the dark blue is 70°C
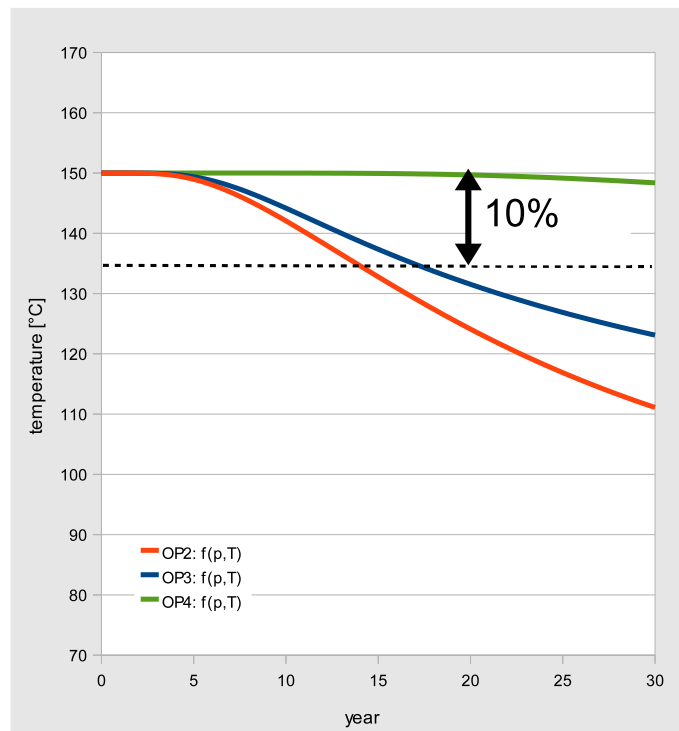

Figure 17: Temperature drop at production wells

4.3 Parameter uncertainty analysis

One of the main tasks of the computer modeling for geothermal systems is prediction of the long-term reservoir performance during heat extraction. Economically desirable characteristics of the reservoirs are, for example, the reservoir life of 15-20 years, and temperature drawdown at the end of the project life < 10% (Baria and Petty, 2008). However, numerical simulations are uncertain because reservoir parameters are derived from limited information and include uncertainties. Influence of parameter uncertainty on the reservoir evaluation has to be investigated for the planning and management of the geothermal resource usage.

The present statistical approach to the uncertainty analysis [EP1] consists of three parts: (1) determination of statistical models for parameter distributions, (2) stochastic realizations of parameter fields using conditional Gaussian simulation based on the defined stochastic models, and (3) Monte-Carlo analysis with numerical simulation of fully coupled THM processes using randomly generalized multiple parameter distributions. Parameters are considered as spatial random variables. Parameter distributions have spatial correlation as well as heterogeneity over the reservoir. As the parameters in principle can be measured in the borehole (i.e. from cores), the parameter values are assumed to be known along the boreholes. The stochastic properties of the random field are given by the probability distribution and spatial correlation.
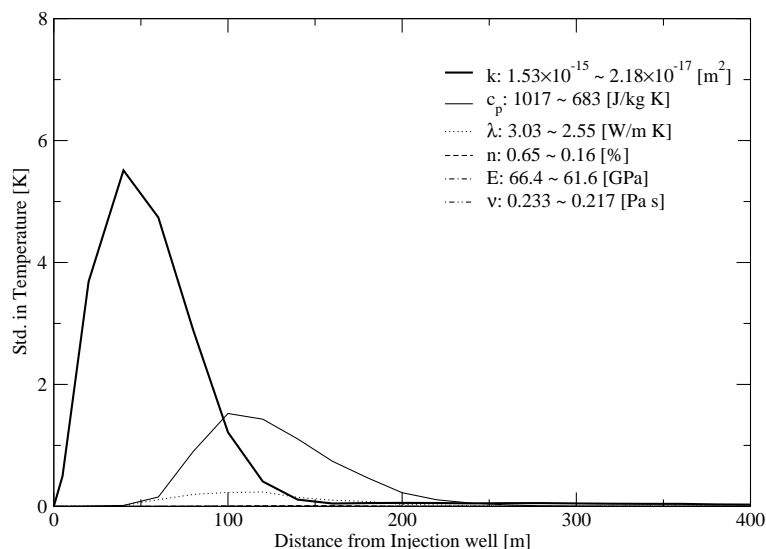

Figure 18: Sensitivity of THM parameters on thermal evolution after 15 years heat extraction

Uncertainty analysis for parameters in THM models was conducted based on data from the geothermal site in Urach Spa. In order to figure out importance of parameter certainty on geothermal reservoir modeling, sensitivity analysis was carried out for parameters in coupled THM models. Study parameters are medium properties (permeability k, porosity n), rock thermal properties (specific heat c_p, heat conductivity λ) and rock mechanical properties (Young's modulus E, Poisson ratio ν). Statistical properties of the parameters are assumed by sampling minimum and maximum value. 10 stochastic simulations were conducted for each parameter. Results of the sensitivity analysis are presented in Figure 18 in terms of standard deviation of predicted temperature profiles after 15 years operation.

The results show uncertainty of permeability makes the strongest variance. Next to permeability, rock specific heat capacity representing heat storage effects, is the second most important parameter. The variances of porosity, Young's modulus, and Poisson ratio are of less importance under the given range in this study.

After the sensitivity analysis, we focus on the effects of hydraulic stimulation on reservoir permeability. As a result of massive hydraulic stimulation, we consider a reservoir type, where hydraulic stimulation is conducted in two boreholes with a quadratic permeability enhancement factor and the porosity-permeability relationship corresponds to that from the Falkenberg site. The mean value of undisturbed permeability is 21.8×10^{-18} m^2 and the standard deviation is 7.17×10^{-18}. Heterogeneity of the undisturbed reservoir is represented using a spherical Variogram model with a correlation length of 50 m range. Hydraulic stimulation is mimicked by a scaling factor between 1 (undisturbed) and 100 (fully stimulated) which is a function of the distance to the borehole. Example of a stochastically generated permeability field is illustrated in Figure 19.
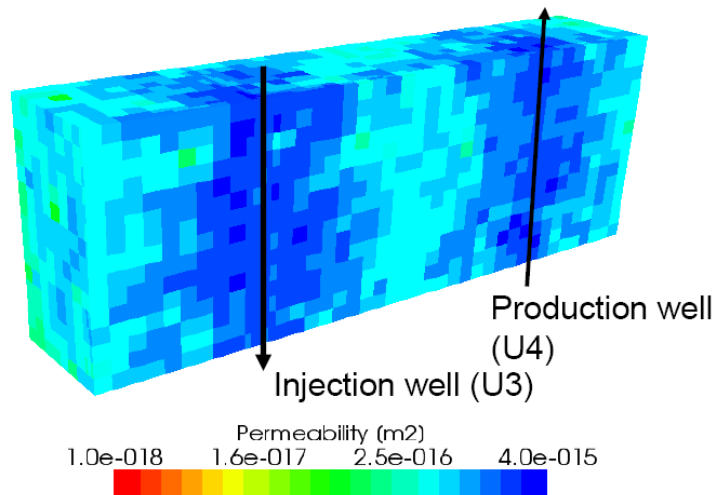

Figure 19: Example of heterogeneous permeability field generated by the stochastic model

To perform a representative Monte-Carlo simulation with the stimulated reservoir, we conduct 100 stochastic simulations. Figure 20 shows result of the Monte-Carlo analysis in terms of uncertainty ranges of temperature profiles in the reservoir after 15 years. Results show a maximum temperature difference of about 40 K at certain place in the reservoir. It can also be seen that the uncertainty, i.e. variance, is largest at places where temperature gradients are highest, i.e. around the propagating cooling front with maximum standard deviation about 8 K. This is because uncertainty of permeability affects the dominating advective heat transport. The results show there is no apparent temperature drop-down at the production well after 15 years heat extraction. However, if the system is operated longer than this period, uncertainty in estimating the end of the project life, i.e. 10 % temperature drop-down, increases because the obtained uncertain range 40 K is nearly 9% of the initial production temperature.

Despite the achievements, the stochastic THM concept has to be further developed in future work. Due to the limited available information, it is difficult to obtain statistical
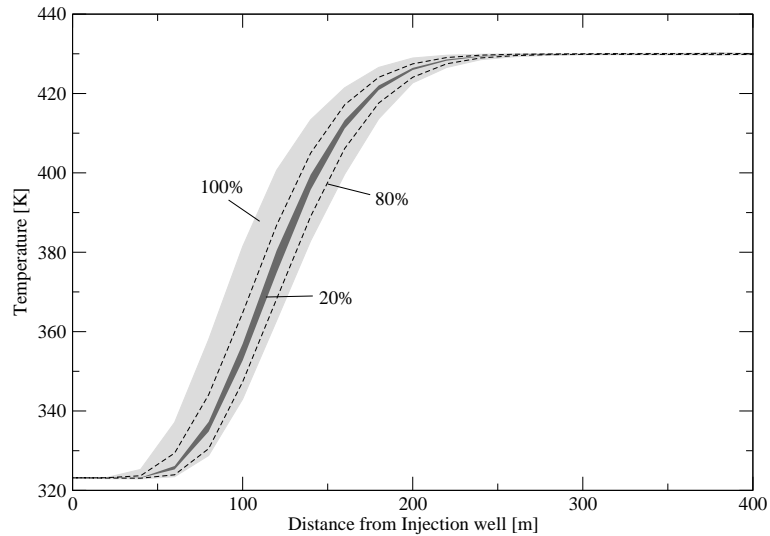
Figure 20: Monte-Carlo analysis: uncertainty ranges of temperature profiles after 15 years heat extraction, 20% (dark gray area), 80% (dotted line), 100% (light gray area)

properties of geothermal HDR reservoirs. Using the Monte-Carlo method, differences in the statistical properties of the spatial distributions will affect the results and potentially bring more uncertainty into the analysis. In addition, it is the fact that parameters are related each other such as porosity-permeability, porosity-rock heat conductivity. The combined parameter variabilities and their effects on reservoir evolution need further investigation. Furthermore, the presented statistical model can be applied only to an equivalent heterogeneous porous medium approach which corresponds to highly fractured reservoirs. The conceptual model of uncertain fractured-porous media requires further development of numerical methods in particular appropriate multi-scale approaches.

4.4 Parallelization

4.4.1 Parallelization of 3D THM problems in porous media

The parallelization scheme presented in section 3.7.2 was applied to solve THM coupled problems in a 3D reservoir model for Urach Spa [EP6]. Hexahedral elements are used in a mesh with 6,600 elements and 7,920 nodes. Figure 21 (left) shows an example of a decomposed mesh for parallel computing with 8 CPUs. Figure 21 (right) shows the decrease of the two different computation times, i.e. CPU time and elapsed time, with increasing numbers of CPUs. With 8 CPUs the both time can be reduced by more than factor 5. A further increasing of CPUs however is not leading to a better parallel performance. The elapsed time with 16 CPUs reduces little and the time with 32 CPUs does not reduce anymore. This is due to two reasons: First, with increasing numbers of domains the inter-processor communication increases, i.e. there is a usual saturation of the speed-up depending on the problem size. For the rather small problem size (6,600 elements) the use of more than 8 CPUs is not sufficient. Second, the job management system is automatically distributing the parallel job on available CPUs which may be located on different nodes. The interconnection between the nodes is a bottleneck for Cluster machines. The used Linux cluster "LiClus" consists of nodes containing 8×DualCore CPUs which are connected via infiniband. The parallel speed-up, therefore, also depends on the distribution of the parallel job
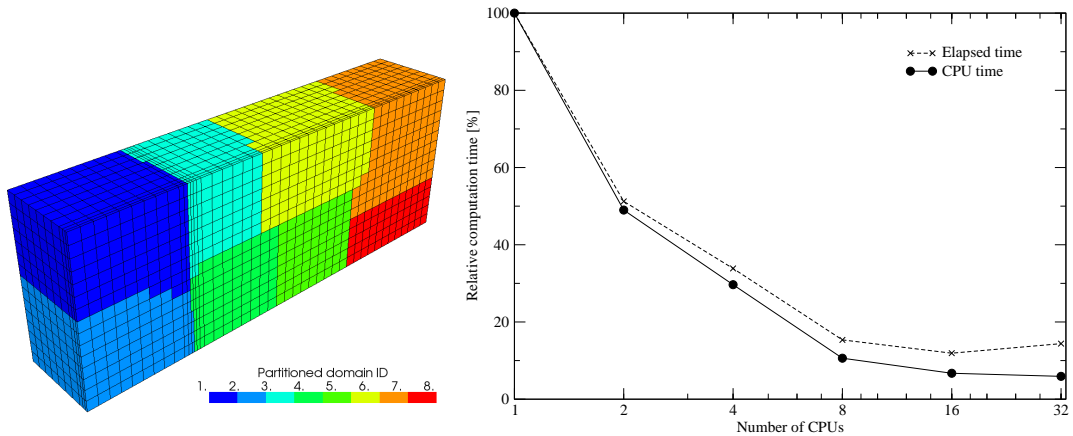
on the cluster nodes.

Figure 21: Domain decomposition for 8 CPUs (left) and improvement of computational time (right)

4.4.2 Parallelization of Monte-Carlo analysis

The uncertainty analysis using a combination of Monte-Carlo simulation and numerical modeling of coupled THM problems is computationally very expensive. Parallel computing is necessary to finish the entire analysis in practical time, including a large number of fully coupled THM simulations. To efficiently use the parallel computing, the analysis can be parallelized in two levels [EP1]. First, simulations of Monte-Carlo method can be conducted in parallel because they are independent processes. Second, in each stochastic simulation, numerical modeling of coupled THM problems can be parallelized as described above. Validity of this approach has been confirmed in the analysis of the uncertainty analysis presented in the previous subsection. For this specific THM problem, the optimum use is exploiting 8 CPUs per parallel job. Therefore, 10 parallel jobs were submitted at the same time to 80 CPUs, i.e. 10 stochastic simulations can be processed in parallel. As a result, the entire Monte-Carlo analysis consisting of 100 statistical realizations could be finished within one day using the parallel cluster instead of 2 months which would have been necessary on a single CPU computer.

5 Conclusions and recommendations

5.1 Conclusions

In this work, the framework of the finite element method (FEM) for coupled thermo-hydro-mechanical (THM) problems in discretely fractured and non-fractured porous media was developed. The model takes into account non-isothermal single-phase flow in deformable porous media connected to discretely fractures. The developed FEM aims to be applied for geotechnical engineering applications such as engineered geothermal systems where discrete fractures play decisive roles to describe heat transport mechanism and subsequent reservoir performance.

Efforts, particularly, have been made for explicit treatment of discrete fractures. In a mathematical standpoint, systems of discretely fractured porous media have to be treated in different ways for hydraulic and heat transport processes, and mechanical process. In hydraulic and heat transport processes, the systems behave like interacted multiple domains, i.e. porous medium domain and discrete fracture domain. In this study, assuming continuity of filed variables (pressure and temperature) over the two domains, superposition of equations for the two distinct systems enables us to solve the equations in one algebraic system. On the other hand, the systems in mechanical process have to take care of displacement discontinuities along discrete fractures. Discrete fractures can be explicitly represented by either conventional interface elements or enrichment methods.

Lower dimensional interface elements with local enrichments have been developed especially for coupled problems in a domain including preexisting fractures. The method developed in this work supports multiple and intersected fractures in two-dimensional space. The method permits the possibility of using existing flow simulators and having an identical mesh for both processes. It gives an advantage in practice that one can use existing standard FEM codes for groundwater flow and easily make a coupling computation between mechanical and hydraulic processes. Example of a 2D fluid injection problem into a single fracture demonstrated that the proposed method can produce results in strong agreement with semi-analytical solutions.

The developed FEM has been applied for uncertainty analysis of the geothermal reservoir behavior. Effects of model parameter uncertainty on long-term geothermal reservoir evolution have been analyzed by the Monte-Carlo method with stochastic models of heterogeneous parameter distributions. The stochastic model has been established mainly based on available data from the Urach Spa. Sensitivity analysis shows that permeability and rock specific heat capacity are the most influential reservoir parameters. Less relevant is rock heat conductivity. The variability of porosity and the mechanical parameters, i.e. Young's modulus and Poisson ratio, in the site specific range is negligible with given parameter ranges.

Numerical modeling of mechanics-related coupled processes in discretely fractured rock is still a big challenge in practice due to the presence of real fracture systems distributed in three-dimensional space. Successful analysis of the system behavior would rely on pre-processing stage, i.e. picking up the most important fractures representing characteristics of the system. In addition, quantification of model uncertainty is almost mandatory for any practical applications.

5.2 Recommendations

The developed FEM has to be further extended to three-dimensional space where discrete fractures distribute. This extension implies also development of robust solvers for both linear and nonlinear equations as well as utilization of parallel computation due to a large number

of degree of freedom and multi-scale physical processes. Extension of lower-dimensional interface elements to three dimensions could be helpful because it allows us to use a single mesh for all coupled process, i.e. helping us to save computational memory and conduct robust calculations due to availability of monolithic coupling.

More complex physical models can be incorporated to simulate various phenomena in subsurface. For example, the non-Darcian flow in fractures has to be taken into account when the flow is not laminar (Kolditz, 2001). Furthermore, fractures could work like an impermeable barrier due to the presence of infill material and it causes pressure variation between two fractures surfaces, i.e. pressure is not continuous anymore over porous medium domains and discrete fracture domains.

Parameter uncertainty analysis can integrate the information about interrelationships between parameters such as porosity-permeability, porosity-rock heat conductivity. Mechanical alternation of porous media could affect not only its structural parameters and hydraulic properties but also thermal properties, which affect performance of geothermal systems. In addition, fractures are uncertain objects themselves as normally only statistical information is available to describe fractures properties such as frequency, size, roughness and fractures aperture distributions. Development of stochastic fractured-porous media models is desirable.

References

Abdelaziz, Y. and Hamouine, A. (2008). A survey of the extended finite element. *Computers & Structures*, 86(11-12):1141–1151.

Alonso, E. E., Alcoverro, J., Coste, F., Malinsky, L., Merrien-Soukatchoff, V., Kadiri, I., Nowak, T., Shao, H., Nguyen, T. S., Selvadurai, A. P. S., Armand, G., Sobolik, S. R., Itamura, M., Stone, C. M., Webb, S. W., Rejeb, A., Tijani, M., Maouche, Z., Kobayashi, A., Kurikami, H., Ito, A., Sugita, Y., Chijimatsu, M., Borgesson, L., Hernelind, J., Rutqvist, J., Tsang, C. F., and Jussila, P. (2005). The FEBEX benchmark test: case definition and comparison of modelling approaches. *International Journal of Rock Mechanics and Mining Sciences*, 42(5-6):611–638.

Baca, R. G., Arnett, R. C., and Langford, D. W. (1984). Modelling fluid flow in fractured-porous rock masses by finite-element techniques. *International Journal for Numerical Methods in Fluids*, 4(4):337–348.

Barenblatt, G., Zheltov, I., and Kochina, I. (1960). Basic concepts in the theory of seepage of homogeneous liquids in fissured rocks (strata). *Journal of Applied Mathematics and Mechanics*, 24:1286–1303.

Baria, R. and Petty, S. (2008). Economic and technical case for commercial exploitation of EGS. In *PROCEEDINGS, Thirty-Third Workshop on Geothermal Reservoir Engineering Stanford University, Stanford, California*.

Bear, J. and Berkowitz, B. (1987). Groundwater flow and pollution in fractured rock aquifers. In Novak, P., editor, *Developments in hydraulic engineering, Volume 4*, pages 175–238. Elsevier, New York.

Belytschko, T. and Black, T. (1999). Elastic crack growth in finite elements with minimal remeshing. *International Journal for Numerical Methods in Engineering*, 45(5):601–620.

Birkholzer, J., Rutqvist, J., Sonnenthal, E., and Barr, D. (2008). DECOVALEX - Task D: Long-term permeability changes due to THC and THM processes. Technical Report 2008:43, Swedish Nuclear Power Inspectorate, Stockholm.

Blöcher, G., Zimmermann, G., and Milsch, H. (2009). Impact of poroelastic response of sandstones on geothermal power production. *Pure and Applied Geophysics*, 166:1107–1123. 10.1007/s00024-009-0475-4.

Blöcher, M. G., Zimmermann, G., Moeck, I., Brandt, W., Hassanzadegan, A., and Magri, F. (2010). 3D numerical modeling of hydrothermal processes during the lifetime of a deep geothermal reservoir. *Geofluids*, 10(3):406–421.

Borja, R. I. and Aydin, A. (2004). Computational modeling of deformation bands in granular media. I. Geological and mathematical framework. *Computer Methods In Applied Mechanics And Engineering*, 193(27-29):2667–2698.

Borsetto, M., Carradori, G., and Ribacchi, R. (1981). Coupled seepage, heat transfer and stress analysis with application to geothermal problems. In Lewis, R. W., Morgan, K., and Zienkiewicz, O. C., editors, *Numerical Methods in Heat Transfer*. Wiley, Chichester.

Bower, K. and Zyvoloski, G. (1997). A numerical model for thermo-hydro-mechanical coupling in fractured rock. *International Journal of Rock Mechanics and Mining Sciences*, 34(8):1201–1211.

Bruel, D. (1995). Modeling heat extraction from forced fluid-flow through stimulated fractured rock masses - evaluation of the Soultz-sous-Forets site potential. *Geothermics*, 24(3):439–450.

Clauser, C. (2003). *Numerical simulation of reactive flows in hot aquifers*. Springer, Berlin / Heidelberg.

Coussy, O. (2004). *Poromechanics*. John Wiley & Sons, Ltd.

Cundall, P. and Hart, R. (1992). Numerical modelling of discontinua. *Engineering Computations*, 9(2):101–113.

de Boer, R. (2005). *Trends in Continuum Mechanics of Porous Media: Theory and Applications of Transport in Porous Media*. Springer-Verlag, Heidelberg.

Dietrich, P., Helmig, R., Sauter, M., Hötzl, H., Köngeter, J., and Teutsch, G., editors (2005). *Flow and Transport in Fractured Porous Media*. Springer-Verlag.

Doughty, C. and Pruess, K. (2004). Modeling supercritical carbon dioxide injection in heterogeneous porous media. *Vadose Zone Journal*, 3:837–847.

Ehlers, W. and Bluhm, J. (2002). *Porous Media: Theory, Experiments and Numerical Applications*. Springer.

Fries, T. and Belytschko, T. (2010). The extended/generalized finite element method: An overview of the method and its applications. *International Journal for Numerical Methods in Engineering*, 84(3):253–304.

Goodman, R. E., Taylor, R. L., and Brekke, T. L. (1968). A model for the mechanics of jointed rock. *Journal of Soil Mechanics and Foundations Div., ASCE*, 94:637–659.

Guimaraes, L. D., Gens, A., and Olivella, S. (2007). Coupled thermo-hydro-mechanical and chemical analysis of expansive clay subjected to heating and hydration. *Transport In Porous Media*, 66(3):341–372.

Guvanasen, V. and Chan, T. (2000). A three-dimensional numerical model for thermo-hydromechanical deformation with hysteresis in a fractured rock mass. *International Journal of Rock Mechanics and Mining Sciences*, 37(1-2):89–106.

Heinicke, J., Fischer, T., Gaupp, R., Götze, J., Koch, U., Konietzky, H., and Stanek, K.-P. (2009). Hydrothermal alteration as a trigger mechanism for earthquake swarms: the Vogtland/NW Bohemia region as a case study. *Geophysical Journal International*, 178(1):1–13.

Jing, L. (2003). A review of techniques, advances and outstanding issues in numerical modelling for rock mechanics and rock engineering. *International Journal of Rock Mechanics and Mining Sciences*, 40(3):283–353.

Karypis, G. and Kumar, V. (1998). A parallel algorithm for multi-level graph partitioning and sparse matrix ordering. *Journal Of Parallel And Distributed Computing*, 48(1):71–95.

Kiryukhin, A., Xu, T., Pruess, K., Apps, J., and Slovtsov, I. (2004). Thermal-hydrodynamic-chemical (THC) modeling based on geothermal field data. *Geothermics*, 33(3):349–381.

Kohl, T. (1992). *Modellsimulation gekoppelter Vorgänge beim Wärmeentzug aus heißem Tiefengestein*. PhD thesis, ETH Zürich.

Kohl, T., Evans, K. F., Hopkirk, R. J., and Rybach, L. (1995). Coupled hydraulic, thermal and mechanical considerations for the simulation of hot dry rock reservoirs. *Geothermics*, 24(3):345–359.

Kohlmeier, M. (2006). *Coupling of thermal, hydraulic and mechanical processes for geotechnical simulations of partially saturated porous media*. PhD thesis, Institut für Strömungsmechanik und Elektron. Rechnen im Bauwesen der Leibniz Universität Hannover.

Kolditz, O. (1995). Modelling flow and heat transfer in fractured rocks: Conceptual model of a 3-D deterministic fracture network. *Geothermics*, 24(3):451–470.

Kolditz, O. (1997). *Strömung, Stoff- und Wärmetransport im Kluftgestein*. Borntraeger, Stuttgart.

Kolditz, O. (2001). Non-linear flow in fractured rock. *International Journal of Numerical Methods for Heat & Fluid Flow*, 11(6):547–576.

Kolditz, O. (2002). *Computational Methods in Environmental Fluid Mechanics*. Springer, Berlin.

Kolditz, O. and de Jonge, J. (2004). Non-isothermal two-phase flow in low-permeable porous media. *Computational Mechanics*, 33(5):345–364.

Korsawe, J., Starke, G., Wang, W., and Kolditz, O. (2006). Finite element analysis of poro-elastic consolidation in porous media: Mixed and standard approaches. *Computer Methods in Applied Mechanics and Engineering*, 195(9-12):1096–1115.

Kuhn, M. (2004). *Reactive Flow Modeling of Hydrothermal Systems*. Springer Berlin / Heidelberg, Lecture Notes in Earth Sciences.

Lehmann, H., Wang, K., and Clauser, C. (1998). Parameter identification and uncertainty analysis for heat transfer at the KTB drill site using a 2-D inverse method. *Tectonophysics*, 291(1-4):179–194.

Lewis, R. W. and Schrefler, B. A. (1998). *The Finite Element Method in the Static and Dynamic Deformation and Consolidation of Porous Media (Second Edition)*. Wiley.

McDermott, C. and Kolditz, O. (2006). Geomechanical model for fracture deformation under hydraulic, mechanical and thermal loads. *Hydrogeology Journal*, 14(4):485–498.

McDermott, C. I., Randriamanjatosoa, A. R., Tenzer, H., and Kolditz, O. (2006). Simulation of heat extraction from crystalline rocks: The influence of coupled processes on differential reservoir cooling. *Geothermics*, 35(3):321–344.

Min, K.-B., Rutqvist, J., Tsang, C.-F., and Jing, L. (2004). Stress-dependent permeability of fractured rock masses: a numerical study. *International Journal of Rock Mechanics and Mining Sciences*, 41(7):1191–1210.

Moës, N., Dolbow, J., and Belytschko, T. (1999). A finite element method for crack growth without remeshing. *International Journal for Numerical Methods in Engineering*, 46(1):131–150.

Ng, K. L. A. and Small, J. C. (1997). Behavior of joints and interfaces subjected to water pressure. *Computers and Geotechnics*, 20(1):71–93.

Noorishad, J., Tsang, C., and Witherspoon, P. (1984). Coupled thermal-hydraulic-mechanical phenomena in saturated fractured porous rocks: numerical approach. *Journal of Geophysical Research*, 89:10365–10373.

Noorishad, J., Tsang, C., and Witherspoon, P. (1992). Theoretical and field studies of coupled hydromechanical behaviour of fractured rocks–1. development and verification of a numerical simulator. *International Journal of Rock Mechanics and Mining Sciences & Geomechanics Abstracts*, 29(4):401–409.

Noorishad, J. and Tsang, C.-F. (1996). Coupled thermohydroelasticity phenomena in variably saturated fractured porous rocks – formulation and numerical solution. In Ove Stephansson, L. J. and Tsang, C.-F., editors, *Coupled Thermo-Hydro-Mechanical Processes of Fractured Media - Mathematical and Experimental Studies*, volume Volume 79, pages 93–134. Elsevier.

Rautman, C. A. and Treadway, A. H. (1991). Geologic uncertainty in a regulatory environment - an example from the potential Yucca Mountain nuclear waste repository site. *Environmental Geology and Water Sciences*, 18(3):171–184.

Rutqvist, J., Barr, D., Birkholzer, J., Chijimatsu, M., Kolditz, O., Liu, Q., Oda, Y., Wang, W., and Zhang, C. (2008). Results from an international simulation study on coupled thermal, hydrological, and mechanical processes near geological nuclear waste repositories. *Nuclear Technology*, 163(1):101–109.

Rutqvist, J. and Stephansson, O. (2003). The role of hydromechanical coupling in fractured rock engineering. *Hydrogeology Journal*, 11(1):7–40.

Schrefler, B. A., Matteazzi, R., Gawin, D., and Wang, X. (2000). Two parallel computing methods for coupled thermohydromechanical problems. *Computer-Aided Civil and Infrastructure Engineering*, 15(3):176–188.

Segura, J. M. and Carol, I. (2004). On zero-thickness interface elements for diffusion problems. *International Journal for Numerical and Analytical Methods in Geomechanics*, 28(9):947–962.

Shioya, R. and Yagawa, G. (2005). Large-scale parallel finite-element analysis using the internet: a performance study. *International Journal for Numerical Methods in Engineering*, 63(2):218–230.

Snow, D. T. (1969). Anisotropie permeability of fractured media. *Water Resources Research*, 5(6):1273–1289.

Stephansson, O., Hudson, J., and Jing, L. (2004). *Coupled Thermo-Hydro-Mechanical-Chemical Processes in Geo-Systems: Fundamentals, Modelling, Experiments, and Applications*. Geo-Engineering Book Series 2. Elsevier.

Strack, O. (1982). Assessment of effectiveness of geologic isolation systems. analytic modeling of flow in a permeable fissured medium. Technical report, Pacific Northwest Lab., Richland, WA.

Taron, J. and Elsworth, D. (2009). Thermal-hydrologic-mechanical-chemical processes in the evolution of engineered geothermal reservoirs. *International Journal of Rock Mechanics and Mining Sciences*, 46(5):855–864.

Taron, J., Elsworth, D., and Min, K.-B. (2009). Numerical simulation of thermal-hydrologic-mechanical-chemical processes in deformable, fractured porous media. *International Journal of Rock Mechanics and Mining Sciences*, 46(5):842–854.

Tenzer, H., Schanz, U., and Homeier, U. (2000). HDR research programme and results of drill hole Urach 3 to depth of 4440 m the key for realisation of a hdr programme in southern Germany and northern Switzerland. *Proceedings World Geothermal Congress 2000*, pages 3927–3932.

Tezduyar, T. E. and Sameh, A. (2006). Parallel finite element computations in fluid mechanics. *Computer Methods in Applied Mechanics and Engineering*, 195(13-16):1872–1884.

Tezuka, K. and Watanabe, K. (2000). Fracture network modeling of Hijiori Hot Dry Rock reservoir by deterministic and stochastic crack network simulator (D/SC). *Proceedings World Geothermal Congress 2000*, pages 3933–3938.

Topping, B. H. V. and Khan, A. I. (1996). *Parallel Finite Element Computations*. Saxe-Coburg Publications, Edinburgh.

Tsang, C. (1991). Coupled hydromechanical-thermochemical processes in rock fractures. *Reviews of Geophysics*, 29(4):537–551.

Walsh, R., McDermott, C., and Kolditz, O. (2008). Numerical modeling of stress-permeability coupling in rough fractures. *Hydrogeology Journal*, 16(4):613–627.

Wang, W., Kosakowski, G., and Kolditz, O. (2009). A parallel finite element scheme for thermo-hydro-mechanical (THM) coupled problems in porous media. *Computers & Geosciences*, 35(8):1631–1641.

Wang, Z. and Konietzky, H. (2009). Modelling of blast-induced fractures in jointed rock masses. *Engineering Fracture Mechanics*, 76(12):1945–1955.

Watanabe, N., Wang, W., Taron, J., Görke, U., and Kolditz, O. (2011). Lower-dimensional interface elements with local enrichment: Application to coupled hydro-mechanical problems in discretely fractured porous media. *International Journal for Numerical Methods in Engineering*. in print.

Weidler, R., Gerard, A., Baria, R., Baumgärtner, J., and Jung, R. (2002). Hydraulic and micro-seismic results of a massive stimulation test at 5km depth at the European Hot-Dry-Rock test site Soultz, France. *Proceedings, 27th Workshop on Geothermal Reservoir Engineering. Stanford, California, January 28-30, 2002*, pages 95–100.

Wijesinghe, A. M. (1986). An exact similarity solution for coupled deformation and fluid flow in discrete fractures. Technical Report UCID–20675, Lawrence Livermore National Laboratory, Livermore, CA.

Woodbury, A. and Zhang, K. (2001). Lanczos method for the solution of groundwater flow in discretely fractured porous media. *Advances in Water Resources*, 24(6):621–630.

Zimmerman, R. W. and Bodvarsson, G. S. (1996). Hydraulic conductivity of rock fractures. *Transport in Porous Media*, 23:1–30.

List of Publications

ISI publications

[**EP1**] **Watanabe, N.**, Wang, W., McDermott, C.I., Taniguchi, T., & Kolditz, O. (2010). Uncertainty analysis of thermo-hydro-mechanical coupled processes in heterogeneous porous media. *Computational Mechanics*, 45, 263-280.

[**EP2**] **Watanabe, N.**, Wang, W., Taron, J., Görke, U.J., & Kolditz, O. (2011). Lower-dimensional interface elements with local enrichment: Application to coupled hydro-mechanical problems in discretely fractured porous media. *International Journal for Numerical Methods in Engineering*, 90(8), 1010-1034.

[**EP3**] Zehner, B., **Watanabe, N.**, & Kolditz, O. (2010). Visualization of gridded scalar data with uncertainty in geosciences. *Computers & Geosciences*, 36(10), 1268-1275.

Peer-reviewed publications

[**EP4**] **Watanabe, N.**, Wang, W., Mcdermott, C. I., & Kolditz, O. (2009). Thermo-Hydro-Mechanical Modelling and Applications for Enhanced Geothermal Reservoirs. *GRC Transactions*, Vol.33 (Vol. 33).

[**EP5**] **Watanabe, N.**, Zehner, B., Wang, W., McDermott, C.I., Taniguchi, T., & Kolditz, O. (2011). Numerical analysis and visualization of uncertainty effects in thermo-hydro-mechanical coupled processes in a hot-dry-rock geothermal reservoir. *Calibration and Reliability In Groundwater Modelling: Managing Groundwater and the Environment, IAHS-AISH Publication*, 341, 57-62, IAHS Press, Wallingford, UK. ISBN 978-1-907161-15-5.

[**EP6**] **Watanabe, N.**, Schnicke T., Wang, W., Wieser, T., & Kolditz, O. (2009) Analysis of Parallelization Efficiency of Coupled Thermo-Hydro-Mechanical Simulation. *Journal of Environmental Science for Sustainable Society*, 3, 50-58. doi:10.3107/jesss.3.50.

Book chapters

[**EP7**] Kolditz, O., Bloecher, M.G., Clauser,C., Diersch, H.-J., Kohl, T., Kuehn, M., McDermott, C.I., Wang, W., **Watanabe, N.**, Zimmermann, G. (2010). Geothermal Reservoir Simulation. In Huenges, E., editor, *Geothermal Energy Systems*. ISBN 978-3-527-40831-3, Wiley-VCH.

[**EP8**] Wang, W., Park, C.-H., **Watanabe, N.**, Kolditz, O. (2012). Numerical methods. In Kolditz, O., Görke, U.-J., Shao, H. and Wang, W., editors, *Benchmarks and Examples for THMC Processes in Porous Media*. LNCSE Monograph Series, Springer Publish, ISBN 978-3-642-27176-2.

[**EP9**] Taron, J., **Watanabe, N.**, Wang, W. (2012). Consolidation processes. In Kolditz, O., Görke, U.-J., Shao, H. and Wang, W., editors, *Benchmarks and Examples for THMC Processes in Porous Media*. LNCSE Monograph Series, Springer Publish, ISBN 978-3-642-27176-2.